Fused heterocycles bearing bridgehead nitrogen as potent HIV-1 NNRTIs. Part 3: Optimization of [1,2,4]triazolo[1,5-a]pyrimidine core via structure-based and physicochemical propert...

13 AUTHORS, INCLUDING:

Huiqing Liu
Shandong University
37 PUBLICATIONS **258** CITATIONS

SEE PROFILE

Christophe Pannecouque
University of Leuven
435 PUBLICATIONS **7,261** CITATIONS

SEE PROFILE

Peng Zhan
Shandong University
134 PUBLICATIONS **1,194** CITATIONS

SEE PROFILE

Xinyong Liu
Shandong University
144 PUBLICATIONS **1,339** CITATIONS

SEE PROFILE

Original article

Fused heterocycles bearing bridgehead nitrogen as potent HIV-1 NNRTIs. Part 3: Optimization of [1,2,4]triazolo[1,5-a]pyrimidine core *via* structure-based and physicochemical property-driven approaches

Boshi Huang [a], Cuicui Li [a], Wenmin Chen [a], Tao Liu [a], Mingyan Yu [b], Lu Fu [a], Yueyue Sun [a], Huiqing Liu [c], Erik De Clercq [d], Christophe Pannecouque [d], Jan Balzarini [d], Peng Zhan [a, *], Xinyong Liu [a, *]

[a] Department of Medicinal Chemistry, Key Laboratory of Chemical Biology (Ministry of Education), School of Pharmaceutical Sciences, Shandong University, 44 West Culture Road, 250012 Ji'nan, Shandong, PR China
[b] Shandong Institute for Food and Drug Control, 2749 Xinluo Street, 250101 Ji'nan, Shandong, PR China
[c] Institute of Pharmacology, School of Medicine, Shandong University, 44 West Culture Road, 250012 Ji'nan, Shandong, PR China
[d] Rega Institute for Medical Research, KU Leuven Minderbroedersstraat 10, B-3000 Leuven, Belgium

ARTICLE INFO

ABSTRACT

In our arduous efforts to develop new potent HIV-1 non-nucleoside reverse transcriptase (RT) inhibitors (NNRTIs), novel piperidine-linked [1,2,4]triazolo[1,5-a]pyrimidine derivatives were designed, synthesized and evaluated for their antiviral activities in MT-4 cell cultures. Biological results showed that all of the title compounds displayed moderate to excellent activities against wild-type (wt) HIV-1 strain (III$_B$) with EC$_{50}$ values ranging from 8.1 nM to 2284 nM in a cell-based assay. Among them, the most promising analog **7d** possessed an EC$_{50}$ value of 8.1 nM against wt HIV-1, which was much more potent than the reference drugs DDI, 3 TC, NVP and DLV. Additionally, **7d** demonstrated weak activity against the double mutant HIV-1 strain (K103N + Y181C), and was more efficient than NVP in a RT inhibition assay. Besides, some measured and calculated physicochemical properties of **7d**, like log P and water solubility, as well as the structure−activity relationships (SARs) analysis have been discussed in detail. Furthermore, the binding mode of the active compound **7d** was rationalized by molecular simulation studies.

© 2015 Elsevier Masson SAS. All rights reserved.

1. Introduction

Acquired immune deficiency syndrome (AIDS) caused by human immunodeficiency virus (HIV), is still a significant pandemic worldwide. Highly active antiretroviral therapy (HAART) has become the most standard and efficient treatment regimen for HIV infection, which generally involves HIV-1 protease inhibitors (PIs) and reverse transcriptase (RT) inhibitors [1]. Among currently available RT inhibitors, non-nucleoside RT inhibitors (NNRTIs) can directly interfere with RT through binding to an allosteric site called NNRTI-binding pocket (NNIBP), which is distinct from, but located at about 10 Å distance from the substrate site [2]. NNRTIs are an important component of the HAART regimen, owing to their unique antiviral activity, high specificity and low cytotoxicity. However, during the clinical use of the first generation NNRTIs (nevirapine, delavirdine and efavirenz), rapid emergence of mutant viral strains severely compromised their application [3–6].

In arduous efforts to explore the resilience of novel NNRTIs to the highly mutable HIV-1, two most representative diarylpyrimidine derivatives (DAPYs) of the second generation of NNRTIs, Etravirine (TMC125, ETR) and Rilpivirine (TMC278, RPV) (Fig. 1) were approved by the US FDA for anti-HIV therapy in 2008 and 2011, respectively, because of their excellent drug resistance profiles [7]. Even so, DAPYs suffer from the severe issues of low oral bioavailability, poor water solubility, cross-resistance, and virologic failure. Thus, the development of new NNRTI drugs with efficient anti-HIV activity against both wild-type (wt) and mutant HIV strains, low cytotoxicity, as well as good pharmacokinetic properties is still urgently required for the successful application of NNRTIs in the drug combination regimens [7].

* Corresponding authors.
    E-mail addresses: zhanpeng1982@sdu.edu.cn (P. Zhan), xinyongl@sdu.edu.cn (X. Liu).
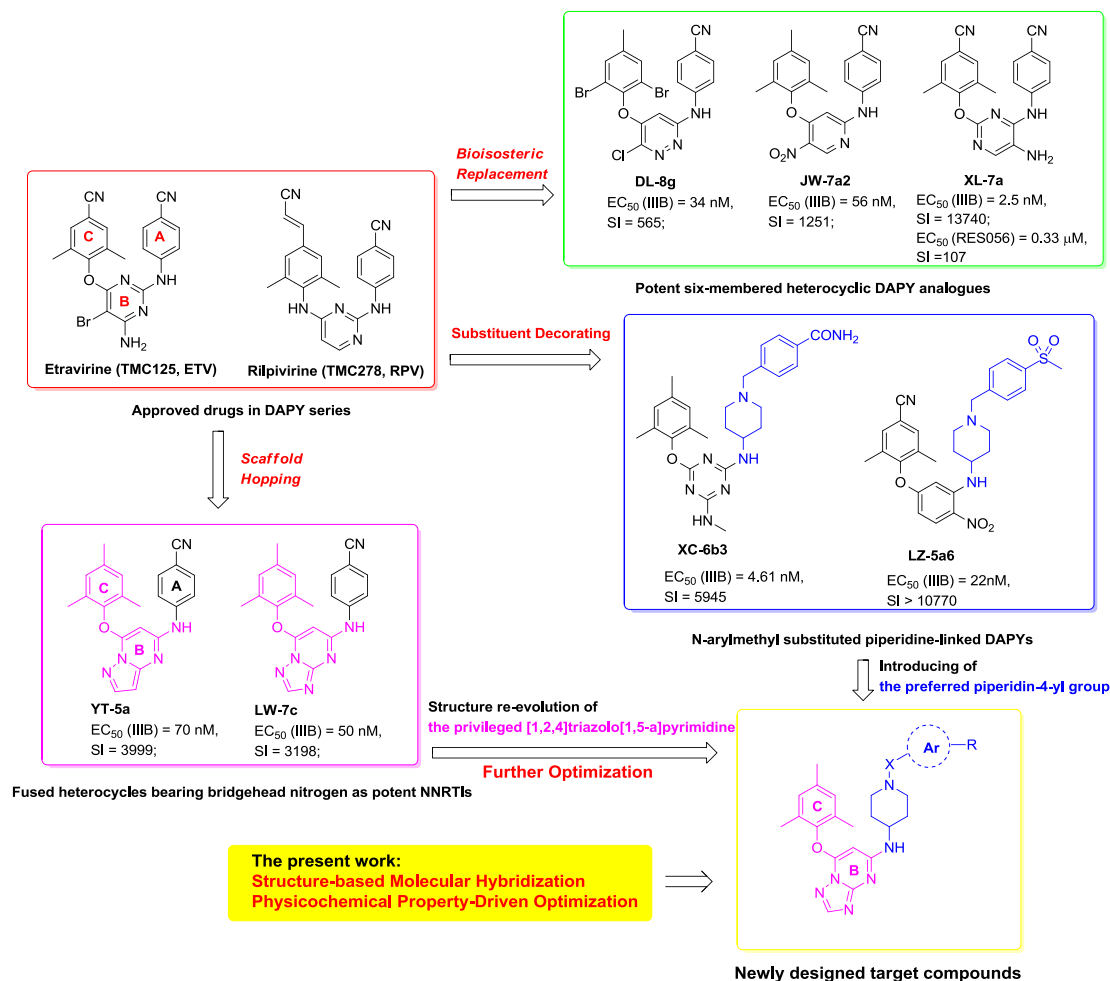
Fig. 1. Graphical representation of our previous work in the structure modifications of DAPY NNRTIs, and optimization strategies for newly designed target compounds in the present work.

Even though confronted with the issues mentioned above, DAPYs, owing to their excellent pharmacological profiles, have still encouraged several research groups to develop next-generation NNRTIs for the treatment of AIDS [8]. As illustrated in Fig. 1, previous research in our laboratory using structure-based bioisosteric replacement, and substituent decoration resulted in the discovery of a collection of six-membered heterocyclic DAPY analogs (exemplified by pyridazine **DL-8g**, nitropyridine **JW-7a2** and pyrimidine **XL-7a**) [9–11], and piperidine-substituted triazine/aniline derivatives (exemplified by **XC-6b3** and **LZ-5a6**) [12–14]. These representative compounds were found to dramatically inhibit the replication of wt HIV-1 strain at low or double-digit nanomolar concentrations (Fig. 1), accompanied with good activity against HIV-1 double mutant strain RES056 (K103N + Y181C), which made them promising leads for further optimization [9–14].

Furthermore, to discover highly potent DAPYs with novel structural motifs that are easier to synthesize or to avoid existing patent art, further modifications were focused in our lab on the replacement of the pyrimidine core in DAPYs with an array of privileged bicyclic scaffolds bearing bridgehead nitrogen [15], such as pyrazolo[1,5-a]pyrimidine **YT-5a** and [1,2,4]triazolo[1,5-a]pyrimidine **LW-7c**, characterized by a 2,4,6-trimethyl group substituted on the **C** ring and a para-cyano group substituted on the **A** ring [16,17]. Interestingly, [1,2,4]triazolo[1,5-a]pyrimidine **LW-7c** demonstrated striking potency against wt HIV-1 strain with an EC_{50}

value of 50 nM, which was much better than Nevirapine (NVP) ($EC_{50} = 150$ nM), and was slightly better than Delavirdine mesylate (DLV) ($EC_{50} = 70$ nM) and its isostere pyrazolo[1,5-a]pyrimidine **YT-5a** ($EC_{50} = 70$ nM). These encouraging results prompted us to evaluate these bicyclic scaffolds during the course of our lead effort for the NNRTI project.

According to the X-ray crystallographic structures of DAPY-RT complexes and the molecular modeling studies [18,19], the binding conformation of DAPYs resembled a characteristic horseshoe or "U" shape in the NNIBP of RT, rather than the prototypical butterfly-like binding shape of the first-generation NNRTIs. The DAPY analogs generally contained three pharmacophoric moieties [2,7]: substituted benzene (**A**) or substituted piperidine in the protein/solvent interface interaction domain, a heterocycle moiety containing a hydrogen bond donor and/or acceptor (**B**) and a hydrophobic group (**C**) (Fig. 1). In particular, the six-membered or bicyclic heterocycle (**B**) located in the center of the NNIBP, not only anchors the functional groups for well engaging with the residues around NNIBP, but also serves as key hydrogen bond acceptor and donor (NH linker) to make key hydrogen bonds with the backbone of K101. These hydrogen bonds are critical for binding affinity of DAPYs especially in the cases of the appearance of K101 mutant [18].

More importantly, crystal structures analysis of piperidine-substituted DAPYs analogs showed that, besides the existing K101

backbone hydrogen bond interactions, the piperidine nitrogen could probably make an additional hydrogen bond with the K103 backbone, which has been considered to be an important factor for the design of inhibitors with resilience to mutations [19]. Moreover, as substituted piperidine points toward the solvent-exposed region, introducing suitable groups into the right-wing piperidine should be beneficial for the modulation of the aqueous solubility, physicochemical and pharmacokinetics properties of the NNRTIs.

On the basis of these analysis and in connection with our previous studies on fused heterocycles bearing bridgehead nitrogen, we continued to explore the privileged and synthetically feasible [1,2,4]triazolo[1,5-a]pyrimidines as more potent anti-HIV agents *via* structure-based molecular hybridization combined with physicochemical property-driven scaffold re-evolution approaches [20]. Concretely, as shown in Fig. 1, the preferred N-(piperidin-4-yl) amine group was installed at the right-wing portion of the [1,2,4] triazolo[1,5-a]pyrimidine core. Meanwhile, different substituents, varying in size and electronic nature were linked to piperidine to further probe the chemical space of the right wing and to establish SARs (Fig. 1).

Herein we report the synthesis, antiviral activity, some measured and calculated physicochemical properties like log P and water solubility of these novel piperidine-linked [1,2,4]triazolo[1,5-a]pyrimidine derivatives. The structure–activity relationships (SARs) are also discussed in detail to gain further insights into this series of analogs.

## 2. Results and discussion

2.1. Chemistry

Newly designed triazolopyrimidine derivatives were expeditiously synthesized *via* a short and efficient route at low cost. As shown in Scheme 1, the starting material 2H-1,2,4-triazol-3-amine (**1**) was first cyclized with the diethyl malonate in dimethyl formamide (DMF), then the reaction mixture was acidified to form the intermediate [1,2,4]triazolo[1,5-a]pyrimidine-5,7-diol (**2**).

Chlorination of **2** with phosphorous oxychloride at 95 °C produced 5,7-dichloro-[1,2,4]triazolo[1,5-a]pyrimidine (**3**) [17]. Coupling of the intermediate **3** with 2,4,6-trimethylphenol using potassium carbonate as the base in DMF at 40 °C gave the intermediate 5-chloro-7-(mesityloxy)-[1,2,4]triazolo[1,5-a]pyrimidine (**4**) [21]. Then the 5-Cl of compound **4** underwent a facile nucleophilic substitution reaction with 4-amino-1-Boc-piperidine in DMF at 60 °C to afford **5** exclusively [12]. Subsequently, intermediate **5** was treated with trifluoroacetic acid (TFA) in dichloromethane solvent at room temperature for 0.5 h to yield the key intermediate **6** [13,14]. Finally, alkylation at the N-1 atom of the piperidinyl group afforded the title compounds **7a–w**, **8a** and **8b** [14]. These target compounds were characterized by physicochemical and spectral means, and both analytical and spectral data of these title compounds were in full agreement with their proposed structures.

2.2. Anti-HIV activity in MT-4 cells

All the newly synthesized compounds were evaluated for their *in vitro* anti-HIV activity and cytotoxicity in MT-4 cells infected with the wild-type HIV-1 (strain IIIB), K103N + Y181C double mutant type HIV-1 (strain RES056), as well as HIV-2 (strain ROD). The biological results, interpreted as EC_{50} values, CC_{50} values and selectivity index (SI) values are summarized in Table 1 and Table 2. Zidovudine (AZT), Didanosine (DDI), Lamivudine (3TC), Nevirapine (NVP), Delavirdine mesylate (DLV), Efavirenz (EFV) and Etravirine (ETR) were used as reference drugs.
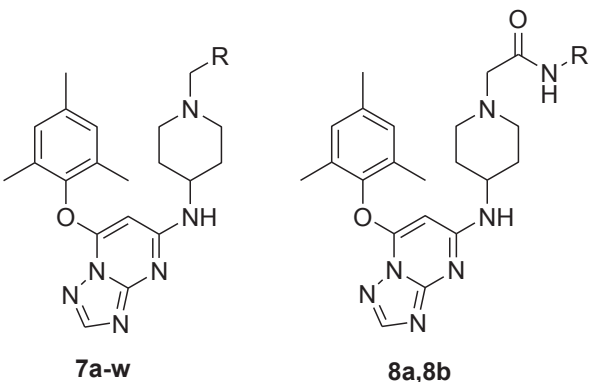
As listed in Table 1, the antiviral activity in the cell-based assay against HIV-IIIB strain of all the newly synthesized compounds were superior to the reference drugs DDI, 3TC and DLV with the exception of compound **8b** (EC_{50} = 2284 nM), and half of these compounds performed better than the lead compound **LW-7c** (EC_{50} = 50 nM). The active derivatives showed moderate to excellent activities with EC_{50} values ranging from 8.1 nM to 2284 nM and SI values in the range of 39–2650. Most notably, compound **7d** was found to be the most potent analog possessing an EC_{50} value of 8.1 nM, much more effective than NVP (EC_{50} = 312 nM) and in the
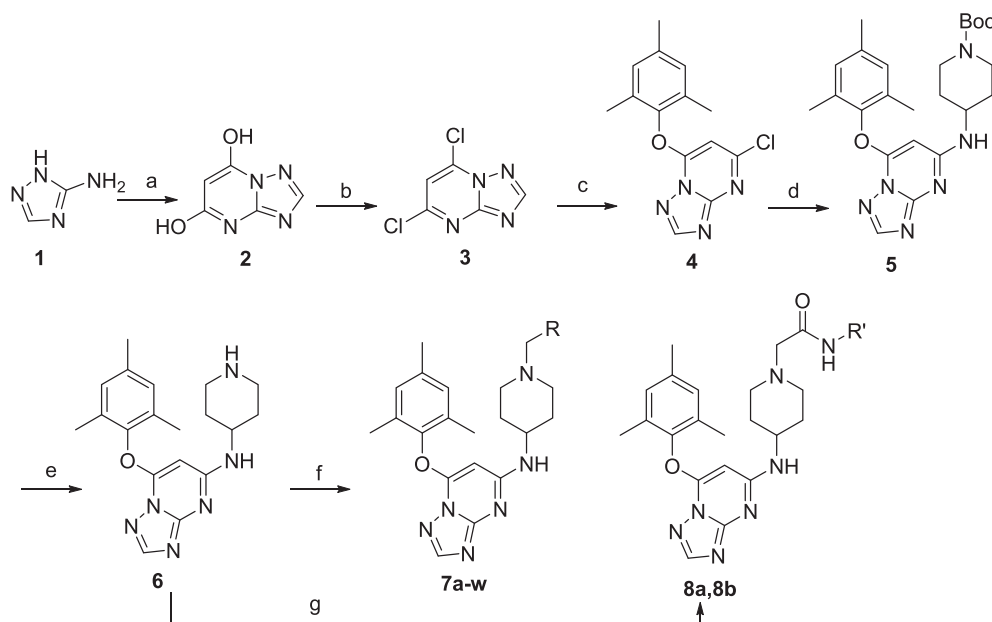
Scheme 1. Reagents and conditions: (a) Diethyl malonate, NaH, DMF, 80 °C, 2 h; (b) POCl₃, 95 °C, 2 h. (c) 2,4,6-trimethylphenol, K₂CO₃, DMF, 40 °C, 2.5 h. (d) *tert*-butyl 4-aminopiperidine-1-carboxylate, K₂CO₃, DMF, 60 °C, overnight. (e) TFA, CH₂Cl₂, r.t., 0.5 h. (f) K₂CO₃, DMF, RCH₂X (X = Cl, Br), r.t., overnight. (g) ClCH₂CONHR′, K₂CO₃, DMF, r.t., overnight.

Table 1

Anti-HIV-1 activity and cytotoxicity of the novel [1,2,4]triazolo[1,5-*a*]pyrimidine compounds in MT-4 cells infected with HIV-1 strain IIIB.

Compd	R/R′	EC_{50} (nM)[a]	CC_{50} (μM)[b]	SI[c]
7a	Cyclohexyl	245 ± 22	13 ± 6.5	50
7b	Pyridin-4-yl	17 ± 9.5	44 ± 18	2650
7c	Phenyl	36 ± 11	25 ± 0.7	708
7d	4-SO_2Me-Ph	8.1 ± 0.8	20 ± 9.3	2548
7e	4-SO_2NH_2-Ph	27 ± 1.9	49 ± 30	1890
7f	4-COOMe-Ph	15 ± 4.6	10 ± 3.7	686
7g	4-NO_2-Ph	35 ± 16	18 ± 2.6	522
7h	4-$CONH_2$-Ph	21 ± 10	24 ± 4.0	1176
7i	4-$COCH_3$-Ph	8.7 ± 1.9	18 ± 9.2	2055
7j	4-Br-Ph	92 ± 59	30 ± 9.4	320
7k	3-Cl-Ph	12 ± 1.3	20 ± 8.9	1643
7l	4-CN-Ph	20 ± 10	14 ± 9.9	689
7m	3-CN-Ph	19 ± 4.1	25 ± 1.9	1324
7n	2-CN-Ph	77 ± 56	27 ± 3.2	356
7o	4-F-Ph	56 ± 8.7	24 ± 1.8	424
7p	3-F-Ph	104 ± 96	≥25	≥238
7q	2-F-Ph	48 ± 11	25 ± 1.9	520
7r	4-CH_3-Ph	72 ± 24	49 ± 32	679
7s	2-CH_3-Ph	42 ± 6.6	24 ± 2.3	590
7t	2,4-di-F-Ph	90 ± 65	23 ± 1.6	255
7u	3,4-di-F-Ph	67 ± 2.1	23 ± 1.8	346
7v	2,5-di-F-Ph	98 ± 19	24 ± 1.0	243
7w	2,6-di-F-Ph	439 ± 188	25 ± 2.1	57
8a	2-Cl-4-COOMe-Ph	277 ± 35	86 ± 22	315
8b	2-Br-4-COOH-Ph	2284 ± 624	89 ± 14	39
LW-7c[d]		50 ± 40	163.8 ± 62.8	3198
AZT		7.1 ± 2.9	>94	>13,144
DDI		23,198 ± 7570	>212	>9
3 TC		2239 ± 826	>87	>39
NVP		312 ± 56	>15	>48
DLV		540 ± 515	>36	>67
EFV		6.3 ± 1.7	>6.3	>1014
ETR		1.8 ± 0.5	4.4 ± 0.8	2459

[a] Compound concentration required to achieve 50% protection of MT-4 cells against HIV-1-induced cytopathic effect, as determined by the MTT method; values are the mean ± SD of at least two parallel tests.
[b] Concentration required to reduce the viability of uninfected cells by 50%, as determined by the MTT method; values were averaged from at least four independent experiments.
[c] Selectivity index: CC_{50}/EC_{50}.
[d] Reference lead used for comparison [17].

Table 2

Anti-HIV activity and cytotoxicity of the novel [1,2,4]Triazolo[1,5-*a*]pyrimidine compounds in MT-4 cells infected with HIV RES056 strain.

Compd	EC_{50} (μM)	FR[a]	CC_{50} (μM)	SI
7a	>13	>50	13 ± 6.5	<1
7b	6.4 ± 3.2	385	44 ± 18	7
7c	>25	>708	25 ± 0.68	<1
7d	13 ± 13	1650	20 ± 9.3	2
7e	22 ± 9.9	838	49 ± 30	2
7f	>10	>686	10 ± 3.7	<1
7g	>18	>522	18 ± 2.6	<1
7h	>24	>1176	24 ± 4.0	<1
7i	>18	>2055	18 ± 9.2	<1
7j	>30	>320	30 ± 9.4	<1
7k	>20	>1643	20 ± 8.9	<1
7l	>14	>689	14 ± 9.9	<1
7m	>25	>1324	25 ± 1.9	<1
7n	>27	>356	27 ± 3.2	<1
7o	>24	>424	24 ± 1.8	<1
7p	≥39	≥372	≥25	≤1
7q	>25	>520	25 ± 1.9	<1
7r	>49	>679	49 ± 32	<1
7s	>24	>590	24 ± 2.3	<1
7t	>23	>255	23 ± 1.6	<1
7u	>23	>346	23 ± 1.8	<1
7v	>24	>243	24 ± 0.96	<1
7w	>25	>57	25 ± 2.1	<1
8a	>86	>315	86 ± 22	<1
8b	>89	>39	89 ± 14	<1
LW-7c [17]	>163.77	>3198	163.77 ± 62.84	<1
AZT	0.010 ± 0.0092	1.4	>94	>9149
DDI	ND	ND	>212	ND
3TC	ND	ND	>87	ND
NVP	≥7.6	≥24	>15	>orX2
DLV	>36	>67	>36	X1
EFV	0.16 ± 0.015	25	>6.3	>41
ETR	0.016 ± 0.0066	8.9	4.4 ± 0.84	277

[a] Fold resistance (FR): ratio of EC_{50} value against K103N + Y181C double mutant type HIV-1 over EC_{50} value against wild-type HIV-1 ($EC_{50}^{mutant}/EC_{50}^{wt}$); data represent the mean ± SD of at least two separate experiments performed in triplicate.

same order of magnitude as those attained for the reference drugs AZT, EFV and ETR. Moreover, **7d** also exhibited an acceptable SI value (2548) *in vitro*. The above biological results demonstrated that introducing a piperidinyl group into [1,2,4]triazolo[1,5-*a*]pyrimidine precursor compound **LW-7c** was acceptable and may improve antiviral potencies.

What is more, these compounds were also assayed against the frequently encountered K103N + Y181C double mutant HIV-1 (strain RES056) in the clinic. As the data indicated in Table 2,

three analogs **7b** (EC_{50} = 6.4 μM with a 385-fold resistance ratio), **7d** (EC_{50} = 13 μM with a 1650-fold resistance ratio) and **7e** (EC_{50} = 22 μM with a 838-fold resistance ratio) displayed weak potency against this mutant strain, which were more active than the reference drug DLV (EC_{50} > 36 μM, fold resistance ratio > 67) and lead compound **LW-7c** (EC_{50} > 163.77 μM, fold resistance ratio > 3198), though still less potent than AZT, EFV and ETR. These acceptable results demonstrated that the replacement of piperidine-substituted groups for benzonitrile in the right wing of the [1,2,4]triazolo[1,5-a]pyrimidine leads did not seriously impair the HIV inhibitory potency and provided new opportunities for further optimization to improve drug resistance profiles. Additionally, all the title compounds were screened for their inhibition against HIV-2 (strain ROD), but like other NNRTIs [9–17], none of them exhibited inhibitory activity at subtoxic concentrations, indicating that this novel series of piperidine-linked [1,2,4]triazolo [1,5-*a*]pyrimidine derivatives were specific for HIV-1 RT.

Based on the results of the biological assays (Table 1), preliminary SARs conclusions could be summarized as follows:

An aromatic ring located at the terminal portion of the right wing of the inhibitors (R substitution) was more beneficial than an aliphatic ring (**7b**, **7c** versus **7a**), and **7b** with a pyridin-4-yl group (EC_{50} = 17 nM) was 2.1 times more active than compound **7c** with a phenyl group (EC_{50} = 36 nM).

Next, we focused our attention on SAR of the *para*-substituents on the phenyl ring (R). Hydrophilic groups were more favorable than hydrophobic groups at the *para* position of the phenyl ring, of which the order ranked as the following: hydrophilic groups [SO_2CH_3 (**7d**, EC_{50} = 8.1 nM) > $COCH_3$ (**7i**, EC_{50} = 8.7 nM) > COOCH_3$

(**7f**, EC$_{50}$ = 15 nM) > CN (**7l**, EC$_{50}$ = 20 nM) ≈ CONH$_2$ (**7h**, EC$_{50}$ = 21 nM) > SO$_2$NH$_2$ (**7e**, EC$_{50}$ = 27 nM)] > H (**7c**, EC$_{50}$ = 36 nM) > hydrophobic groups [F (**7o**, EC$_{50}$ = 56 nM) > CH$_3$ (**7r**, EC$_{50}$ = 72 nM) > Br (**7j**, EC$_{50}$ = 92 nM)], except for **7g** with a hydrophobic NO$_2$ group (EC$_{50}$ = 35 nM) similar to **7c** (EC$_{50}$ = 36 nM). The antiviral activity of **7i** was nearly as high as the most potent compound **7d** bearing SO$_2$CH$_3$ as a classical bioisostere of COCH$_3$, suggesting that the sulfuryl/carbonyl group with appropriate polarity and hydrophilicity can better accommodate the chemical environment in this region of RT and provide potential interactions with surrounding amino acids. This conclusion was in agreement with the previously reported results in the piperidine-substituted series.

Moreover, the influence of substituents at the *ortho* or *meta* position of the phenyl ring (R) on the antiviral activity was investigated, but no distinct features were exhibited in this case (**7l** versus **7m** versus **7n**; **7o** versus **7p** versus **7q**; **7r** versus **7s**).

Considering the fact that the introduction of a fluorine atom to bioactive molecules could significantly affect on pharmaceutical profiles such as activity, metabolism and physicochemical properties including lipophilicity and solubility. Thus, multiple fluorine atoms were also introduced to the benzyl moiety, which resulted in compounds **7t**–**7w**. Unfortunately, the four di-F-substituted analogous merely showed moderate anti-HIV-1 profiles, and did not demonstrate remarkable advantages over the single fluorine-containing compounds **7o**–**q**.

Finally, to further probe the chemical space of the right wing in the protein/solvent interface of RT, the substituted acetanilide motif, a dominating element in arylazolyl(azinyl)thioacetanilide-typed NNRTIs [22], was linked to the piperidine-NH, resulting in compounds **8a** and **8b**. Unfortunately, both of them displayed significantly impaired anti-HIV-1 activity, which were inferior to all of the derivatives in series **7** with the exception of **7w**. This result indicated that the length and size of the linker between piperidine-NH and the terminal phenyl ring should be appropriate, to make compounds well adopted in the NNIBP of HIV-1 RT. In brief, the detailed SAR concluded above provides valuable information for further rational design of this type of HIV-1 NNRTIs.

2.3. Inhibition of HIV-1 RT

To further confirm that the title compounds target HIV-1 RT, the most active compound **7d** was tested in recombinant HIV-1 RT inhibitory assays which use poly (A) × oligo (dT)$_{15}$ as template/primer (RT kit, Roche). As shown in Table 3, compound **7d** exhibited moderate activity against HIV-1 RT with an IC$_{50}$ value of 0.50 μM, which was comparable to that of NVP (IC$_{50}$ = 0.58 μM), while inferior to that of ETR (IC$_{50}$ = 0.089 μM). The results further indicated that the newly synthesized compounds, represented by compound **7d**, could effectively inhibit the activity of HIV-1 RT, thus acting as typical HIV-1 NNRTIs.

2.4. Molecular modeling analysis

To better understand the interactions between the newly

Table 3
Inhibitory activity of compound **7d**, NVP and ETR against HIV-1 RT.[a]

Compd	7d	NVP	ETR
IC$_{50}$ (μM)[b]	0.50	0.58	0.089

[a] The RT kit was commercially available and supplied by Roche, and data were obtained by standard ELISA.
[b] The inhibitory concentration of the tested compounds required to inhibit biotin deoxyuridine triphosphate (biotin-dUTP) incorporation into the HIV-1 RT by 50%.

synthesized compounds and RT, and to rationalize the results of SAR studies, molecular modeling was carried out to investigate the binding mode of target compounds. The representative compound **7d** and the lead compound **LW-7c** were docked into the NNIBP of HIV-1 RT (PDB code: 3M8Q [19,23]) by Surflex-Dock module of Sybyl-X 1.1 software [24] and the docking results were shown by PyMOL 1.5. Default parameters were used as described in the SYBYL-X 1.1 manual unless otherwise specified.

As illustrated in Fig. 2a–c, the binding mode of compound **7d** is similar to that of **LW-7c**, as observed by a fair superimposition of
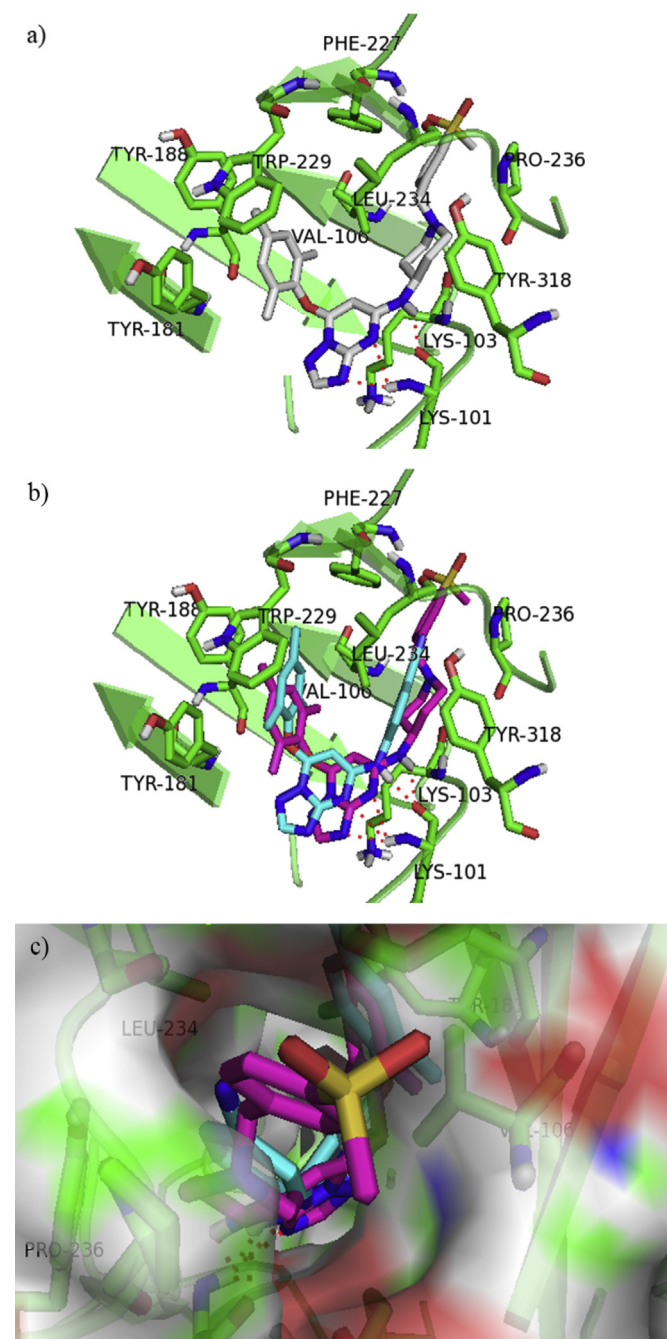

Fig. 2. (a) Model of **7d** docked into RT wt (PDB code: 3M8Q); (b) and (c) Superimposition of the docked conformations of **7d** (magenta) and lead **LW-7c** (cyan) in RT wt (PDB code: 3M8Q). Hydrogen bonds are indicated with dashed lines in red, and all the hydrogen atoms are omitted for clarity. (For interpretation of the references to colour in this figure legend, the reader is referred to the web version of this article.)

their docked conformation. Particularly, their common binding pattern can be described as follows: 1) The left wing of the compounds fits into the aromatic-rich binding sub-pocket, which is formed by the aromatic side chains of Tyr188, Tyr181, Phe227, and Trp229. The 2,4,6-trimethyl-substituted phenoxyl group is parallel to the side-chain phenyl group of Tyr181, exhibiting positive Van der Waals interactions. 2) $3'$-N and $5'$-N of [1,2,4]triazolo[1,5-a] pyrimidine core in **7d** form two hydrogen bonds with backbone α-amino, besides, *NH* forms another one with backbone carbonyl of residue Lys101, whereas lead compound **LW-7c** only forms two hydrogen bonds with residue Lys101. 3) The extra piperidinyl group incorporated to enhance the binding affinity and to optimize the inhibitors' water solubility (will be evidenced by measurement in the next section) locates around amino acids Tyr318, Leu234 and Val106, which can be well adopted in the NNIBP. Additionally, the polar hydrophilic substituent −SO₂Me group resides between Val106 and Pro236 and is oriented directly toward a solvent exposure region (Fig. 2c). Therefore, **7d** probably reserves a tighter interaction with RT than **LW-7c**, which may contribute to the higher anti-HIV-1 activity of **7d** as compared to compound **LW-7c**.

Overall, the binding model analysis confirmed our original design hypothesis that introducing a piperidinyl group into the right-wing portion of [1,2,4]triazolo[1,5-a]pyrimidines could make terminal phenyl ring of new compounds to extend more closer to the protein/solvent interface of HIV-1 RT. These aspects will be taken into account for further structural optimization.

2.5. In silico calculation of physicochemical properties and measured log P and water solubility

Because of hydrophobic nature of the NNRTIs binding site, the high biological potency of current DAPY derivatives (including the approved TMC125 and TMC278) is often compromised by poor water solubility. Poor aqueous solubility often leads to inconclusive biological assay results, undesirable ADME properties, such as limited molecular absorption and low oral bioavailability, high dosages, and difficulties in formulation, which hinder further drug development. Therefore, molecular water solubility was considered as a major factor evaluating the quality of a drug candidate [25]. To investigate whether the additional piperidine group could enhance aqueous solubility of the new compounds, we further investigated water solubility and other physichemical properties for the representative compound **7d** in parallel with the reference drug **ETR**, as shown in Table 4. The results of physicochemical properties revealed that **7d** and **ETR** agreed well with the Lipinski's rule of five. The experimental data indicated that **7d** has a favorable log P value. More importantly, **7d** was much more water-soluble than **ETR**. Thus, compound **7d** has a better balance of favorable activity against wt HIV-1 and reasonable drug-like properties, which seems to make it a promising lead for further optimization.

3. Conclusions

Briefly, based on the structure of the previously reported DAPY-like lead compound **LW-7c** with a bridgehead nitrogen 1,2,4-triazolo[1,5-a]pyrimidine core, we designed and synthesized a series of novel NNRTIs by employing structure-based molecular hybridization combined with physicochemical property-driven scaffold re-evolution approaches. Intriguingly, most of the target compounds showed moderate to excellent anti-HIV-1 potency. Half of these newly synthesized inhibitors exhibited antiviral profiles superior to that of **LW-7c** and much better than those of DDI, NVP and DLV. Among them, **7d** was identified as the most promising compound in inhibiting wt HIV-1 (IIIB) replication with an EC_{50} value of 8.1 nM, which was prior to **LW-7c** and much better than those of the reference drugs DDI (EC_{50} = 23,198 nM), 3TC (EC_{50} = 2239 nM), NVP (EC_{50} = 312 nM) and DLV (EC_{50} = 540 nM). In addition, **7d** showed weak activity against the double mutant HIV-1 strain RES056 (K103N + Y181C), and could inhibit HIV-1 RT more efficient than NVP. Furthermore, the preliminary SAR and molecular modeling studies were carried out to assess the interactions between these inhibitors and HIV-1 RT. Some physicochemical properties like log P and water solubility of **7d** were also measured. These valuable information provide us deeper insight into these promising structures, and further efforts to improve the antiviral activity of these piperidine-linked derivatives will be reported in due course.

4. Experimental section

4.1. Chemistry

All melting points were measured with a micromelting point apparatus and are uncorrected. ¹H NMR and ¹³C NMR spectra were obtained on a Bruker AV-400 spectrometer (Bruker BioSpin, Switzerland), or Bruker AVANCE-300 spectrometer (Bruker Bio-Spin, Switzerland), using tetramethylsilane (TMS) as internal reference. The solvent used was DMSO-d_6 unless otherwise indicated. Chemical shifts were expressed in δ units (ppm) and J values were presented in hertz (Hz). Mass spectrometry was performed on an LC Autosampler Standard G1313A instrument (Applied Biosystems/MDS Sciex, Concord, ON, Canada). TLC was performed on pre-coated HUANGHAI HSGF254, 0.15−0.2 mm TLC-plates (Yantai Jiangyou Silica Gel Development Co., Ltd, Yantai, Shandong, PR China), and spots were visualized by irradiation with UV light (λ 254 nm). Flash column chromatography was performed on columns packed with silica gel 60 (200−300 mesh) (Qingdao waves silica gel desiccant co., Ltd, Qingdao, PR China). Solvents were of reagent grade, and if necessary, were purified and dried by standard methods. The key reagents were purchased from commercial suppliers and without further purification when used. Rotary evaporators served in concentration of the reaction solutions at reduced pressure.

4.1.1. General procedure for the synthesis of 7-(mesityloxy)-N-(piperidin-4-yl)-[1,2,4]triazolo[1,5-a]pyrimidin-5-amine (6)

[1,2,4]triazolo[1,5-a]pyrimidine-5,7-diol (**2**): NaH (5.71 g,

Table 4
Physicochemical properties[a] and water solubility of **7d** and **ETR**.

Items of physicochemical properties	Acceptable range	7d	ETR
EC_{50}(nM)		8.1	1.8
natoms		37	28
MW	<500 Da	520.65	435.28
nON	<10	9	7
nOHNH	<5	1	3
nrotb	≤10	7	4
tPSA	<140 Å²	101.732	120.65
MV		465.592	335.95
Log P	<5	1.91[b]	>5[c]
nViol		1	1
Solubility in water (pH = 7) (μg/mL)		10.31[d]	<<1[c]

[a] Using free on-line software (http://www.molinspiration.com/); natoms = number of atoms; MW = molecular weight; nON = no. of hydrogen bond acceptors; nOHNH = no. of hydrogen bond donors; nrotb = no. of rotatable bonds; tPSA = topological polar surface area, as a prediction of oral bioavailability; MV = molar volume; log P = logarithm of partition coefficient; nViol = no. of violations.
[b] Values were measured at pH 7 by HPLC method in duplicate.
[c] See Ref. [26].
[d] Measured in water at pH 7 by HPLC method in duplicate.

238 mmol) was added in portions to a solution of 1*H*-1,2,4-triazol-5-amine (**1**) (10.00 g, 119 mmol), diethyl malonate (22.86 g, 143 mmol) in redistilled DMF (50 mL) at room temperature. The mixture was stirred at 80 °C for 2 h, and the solution was partially solidified. Then, H_2O (150 mL) was added, and the mixture was washed with EtOAc (3 × 30 mL). The aqueous layer was separated, and then adjusted to pH 1.0 with 8N HCl in an ice bath. The resultant solid was filtered, washed with water, and dried under vacuum to give [1,2,4]triazolo[1,5-*a*]pyrimidine-5,7-diol (**2**) as a white solid. Yield: 77%, mp: 238–240 °C. ESI-MS: *m/z* 151.1 (M−1).

5,7-dichloro-[1,2,4]triazolo[1,5-*a*]pyrimidine (**3**): Intermediate **2** (1.00 g, 6.6 mmol) was added to phosphorous oxychloride ($POCl_3$) (6.2 mL, 66 mmol) and refluxed at 95 °C for 2 h in a round bottom flask, during which the solution turned dark. Excess $POCl_3$ was removed under reduced pressure and the residue was treated with triturated ice. Potassium carbonate (K_2CO_3) was slowly added into this ice-water solution to adjust the pH to 8.0 in an ice bath. The mixture was extracted with dichloromethane (CH_2Cl_2) (3 × 20 mL). Then the combined organic layers were washed with saturated brine (30 mL), subsequently dried over anhydrous Na_2SO_4, filtered and concentrated to give the crude product 5,7-dichloro-[1,2,4] triazolo[1,5-*a*]pyrimidine (**3**) as a yellow solid. **3** could be used in the next step without further purification. Yield: 64%, mp:126–130 °C. ESI-MS: *m/z* 189.3 (M+1), 191.3 (M+3), 193.2 (M+5).

tert-butyl-4-((7-(mesityloxy)-[1,2,4]triazolo[1,5-*a*]pyrimidin-5-yl)amino)piperidine-1-carboxylate (**5**): K_2CO_3 (1.46 g, 10.58 mmol) was slowly added to a solution of 2,4,6-trimethylphenol (0.72 g, 5.3 mmol) in redistilled DMF (10 mL). The mixture was stirred at room temperature for 10 min, then intermediate **3** (1.00 g, 5.3 mmol) was added. The reaction was heated at 40 °C for 2.5 h until its completion. After that, 4-amino-1-Boc-piperidine (1.17 g, 5.8 mmol), K_2CO_3 (0.73 g, 5.3 mmol) and redistilled DMF (4.0 mL) were added into above solution, and then the reaction mixture was stirred at 60 °C overnight. Then, DMF was evaporated under reduced pressure and H_2O (30 mL) was added to the residue. The aqueous solution was extracted with EtOAc (3 × 30 mL). The combined organic layer was washed with saturated brine (40 mL) and dried over anhydrous Na_2SO_4, filtered and concentrated under reduced pressure. Purification by flash column chromatography and recrystallization of the residue gave intermediate **5** as a white solid. Two-step total yield: 34%, mp: 240–242 °C. ESI-MS: *m/z* 453.6 (M+1), 475.5 (M+23).

7-(mesityloxy)-*N*-(piperidin-4-yl)-[1,2,4]triazolo[1,5-*a*]pyrimidin-5-amine (**6**): To a solution of **5** (1.05 g, 2.3 mmol) in CH_2Cl_2 (3.0 mL), trifluoroacetic acid (TFA, 3.0 mL) was added dropwise. The reaction mixture was stirred for 0.5 h at room temperature. After removal of the excess solvent under reduced pressure, saturated K_2CO_3 aqueous solution (10 mL) was added. The resultant precipitate was filtered, washed by water and dried in vacuum to give the key intermediate **6** as a white solid. Yield: 86%, decomposed (below the mp). ESI-MS: *m/z* 353.5 (M+1), 375.4 (M+23).

4.1.2. General procedure for the synthesis of target compounds **7a**−**7w** and **8a**, **8b**

At room temperature, key intermediate **6** (0.20 g, 0.57 mmol) and anhydrous K_2CO_3 (0.16 g, 1.14 mmol) were added to anhydrous DMF (5 mL), followed by the addition of the appropriate RCH₂X (X = Cl, Br) or ClCH₂CONHR'(0.63 mmol). Then the reaction mixture was stirred overnight at room temperature. The solvent was evaporated under reduced pressure, and H_2O (30 mL) was added. After extraction with CH_2Cl_2 or EtOAc (3 × 30 mL), the combined organic phase was washed with saturated brine (40 mL), dried over anhydrous Na_2SO_4, filtered and concentrated under reduced pressure. Then the residue was further purified by flash column

chromatography and subsequently recrystallized with anhydrous methanol to afford pure title compounds **7a**−**7w** and **8a**, **8b**.

*4.1.2.1. N-(1-(cyclohexylmethyl)piperidin-4-yl)-7-(mesityloxy)-[1,2,4]triazolo[1,5-a]pyrimidin-5-amine (**7a**).* White solid, yield: 46%. mp: 249–250 °C. [¹H] NMR (300 MHz, DMSO-d_6, ppm) δ: 8.16 (s, 1H, triazole-H), 7.49 (d, *J* = 7.50 Hz, 1H, NH), 7.07 (s, 2H, OPh-H), 5.31 (s, 1H, pyrimidine-H), 3.78–3.76 (m, 1H, piperidine-H), 2.71 (d, *J* = 11.70 Hz, 2H, piperidine-H), 2.30 (s, 3H, CH_3), 2.09 (s, 6H, CH_3 ×2), 2.06–2.03 (m, 2H, piperidine-H), 2.00–1.93 (m, 2H, hex-H), 1.84 (d, *J* = 11.10 Hz, 2H, CH_2), 1.72–1.62 (m, 5H, piperidine-H, hex-H), 1.44–1.40 (m, 1H, hex-H), 1.39–1.28 (m, 2H, piperidine-H), 1.27–1.05 (m, 3H, hex-H), 0.85–0.74 (m, 2H, hex-H). [¹³C] NMR (75 MHz, DMSO-d_6, ppm) δ: 160.08, 157.29, 153.98, 152.67, 145.93, 136.15, 129.99, 129.49, 79.19, 64.98, 52.34, 47.49, 34.67, 31.30, 26.36, 25.52, 20.29, 15.24. ESI-MS: *m/z* 449.5 (M+1), 450.6 (M+2), $C_{26}H_{36}N_6O$ (448.60).

*4.1.2.2. 7-(Mesityloxy)-N-(1-(pyridin-4-ylmethyl)piperidin-4-yl)-[1,2,4]triazolo[1,5-a] pyrimidin-5-amine (**7b**).* White solid, yield: 34%. mp: 257–258 °C. [¹H] NMR (400 MHz, DMSO-d_6, ppm) δ: 8.50 (dd, *J* = 4.52 Hz,1.36 Hz, 2H, pyridine-3′,5′-H), 8.18 (s, 1H, triazole-H), 7.55 (d, *J* = 7.20 Hz, 1H, NH), 7.31 (d, *J* = 5.76 Hz, 2H, pyridine-2′, 6′-H), 7.08 (s, 2H, PhH), 5.32 (s, 1H, pyrimidine-H), 3.83–3.82 (m, 1H, piperidine-H), 3.49 (s, 2H, CH_2), 2.72 (d, *J* = 11.46 Hz, 2H, piperidine-H), 2.30 (s, 3H, CH_3), 2.15–2.12 (m, 2H, piperidine-H), 2.09 (s, 6H, CH_3×2), 1.88 (d, *J* = 10.40 Hz, 2H, piperidine-H), 1.44–1.36 (m, 2H, piperidine-H). [¹³C] NMR (100 MHz, DMSO-d_6, ppm) δ: 160.57, 157.77, 154.50, 153.19, 149.98, 148.24, 146.41, 136.67, 130.50, 130.00, 124.10, 79.68, 61.24, 52.23, 47.62, 31.68, 20.80, 15.75. ESI-MS: *m/z* 444.6 (M+1),466.5 (M+23), $C_{25}H_{29}N_7O$ (443.54).

*4.1.2.3. N-(1-benzylpiperidin-4-yl)-7-(mesityloxy)-[1,2,4]triazolo[1,5-a]pyrimidin-5-amine (**7c**).* White solid, yield: 48%. mp: 236.5–237 °C. [¹H] NMR (300 MHz, DMSO-d_6, ppm) δ: 8.17 (s, 1H, triazole-H), 7.52 (d,*J* = 7.20 Hz, 1H, PhH), 7.34–7.21 (m, 5H, NH and PhH), 7.07 (s, 2H, OPh-H), 5.32 (s, 1H, pyrimidine-H), 3.82–3.80 (m, 1H, piperidin-H), 3.45 (s, 2H, CH_2), 2.73 (d, *J* = 11.10 Hz, 2H, piperidin-H), 2.30 (s, 3H, CH_3), 2.09–2.04 (m, 8H, piperidin-H, CH_3), 1.86 (d,*J* = 10.20 Hz, 2H, piperidin-H), 1.42–1.32 (m, 2H, piperidin-H). [¹³C] NMR (75 MHz, DMSO-d_6, ppm) δ: 160.08, 157.29, 153.98, 152.69, 145.94, 138.56, 136.15, 129.99, 129.49, 128.69, 128.09, 126.78, 79.21, 62.16, 51.66, 47.31, 31.23, 20.29, 15.23. ESI-MS: *m/z* 443.7 (M+1), $C_{26}H_{30}N_6O$ (442.56).

*4.1.2.4. 7-(Mesityloxy)-N-(1-(4-(methylsulfonyl)benzyl)piperidin-4-yl)-[1,2,4]triazolo [1,5-a]pyrimidin-5-amine (**7d**).* White solid, yield: 45%. mp: 258–259 °C. [¹H] NMR (400 MHz, DMSO-d_6, ppm) δ: 8.17 (s, 1H, triazole-H), 7.88 (d, *J* = 8.28 Hz, 2H, PhH), 7.57 (d, *J* = 8.24 Hz, 2H, PhH), 7.54 (d, *J* = 7.24 Hz, 1H, NH), 7.08 (s, 2H, OPh-H), 5.32 (s, 1H, pyrimidine-H), 3.83–3.82 (m, 1H, piperidine-H), 3.57 (s, 2H, CH_2), 3.20 (s, 3H, SO_2CH_3), 2.73 (d, *J* = 11.36 Hz, 2H, piperidine-H), 2.30 (s, 3H, CH_3), 2.16–2.13 (m, 2H, piperidine-H), 2.09 (s, 6H, CH_3 ×2), 1.88 (d,*J* = 10.36 Hz, 2H, piperidine-H), 1.43–1.35 (m, 2H, piperidin-H). [¹³C] NMR (100 MHz, DMSO-d_6, ppm) δ: 160.57, 157.77, 154.50, 153.20, 146.42, 145.45, 139.83, 136.68, 130.50, 130.00, 129.79, 127.40, 79.69, 61.88, 52.21, 47.67, 44.06, 31.70, 20.80, 15.75. ESI-MS: *m/z* 521.5 (M+1), 543.5 (M+23), $C_{27}H_{32}N_6O_3S$ (520.65).

*4.1.2.5. 4-((4-((7-(Mesityloxy)-[1,2,4]triazolo[1,5-a]pyrimidin-5-yl)amino)piperidin-1-yl)methyl)benzenesulfonamide (**7e**).* White solid, yield: 38%. mp: 319–319.5 °C. [¹H] NMR (300 MHz, DMSO-d_6, ppm) δ: 8.17 (s, 1H, triazole-H), 7.78 (d, *J* = 7.80 Hz, 2H, PhH), 7.53 (d, *J* = 7.50 Hz, 1H, NH), 7.48 (d, *J* = 8.10 Hz, 2H, PhH), 7.29 (s, 2H, SO_2NH_2), 7.08 (s, 2H, OPh-H), 5.32 (s, 1H, pyrimidine-H), 3.82 (m,

1H, piperidine-H), 3.53 (s, 2H, CH₂), 2.72 (d, *J* = 10.80 Hz, 2H, piperidine-H), 2.30 (s, 3H, CH₃), 2.14−2.09 (m, 8H, piperidine-H, CH₃), 1.87 (d, *J* = 10.50 Hz, 2H, piperidine-H), 1.43−1.33 (m, 2H, piperidine-H). ¹³C NMR (75 MHz, DMSO-*d₆*, ppm) δ: 160.59, 157.78, 154.49, 153.21, 146.44, 143.34, 143.17, 136.67, 130.50, 130.00, 129.45, 126.07, 79.71, 61.95, 52.16, 47.72, 31.69, 20.79, 15.74. ESI-MS: *m/z* 522.5 (M+1), 544.5 (M+23), C₂₆H₃₁N₇O₃S (521.63).

*4.1.2.6. Methyl-4-((4-((7-(mesityloxy)-[1,2,4]triazolo[1,5-a]pyrimidin-5-yl)amino) piperidin-1-yl)methyl)benzoate (**7f**).* White solid, yield: 35%. mp: 240.5−241 °C. ¹H NMR (300 MHz, DMSO-*d₆*, ppm) δ: 8.17 (s, 1H, triazole-H), 7.92 (d, *J* = 8.10 Hz, 2H, PhH), 7.52 (d, *J* = 6.90 Hz, 1H, NH), 7.45 (d, *J* = 8.10 Hz, 2H, PhH), 7.08 (s, 2H, OPh-H), 5.32 (s, 1H, pyrimidine-H), 3.84 (s, 4H, COOCH₃ and piperidine-H), 3.53 (s, 2H, CH₂), 2.72 (d, *J* = 11.10 Hz, 2H, piperidine-H), 2.30 (s, 3H, CH₃), 2.15−2.09 (m, 8H, piperidine-H, CH₃), 1.87 (d, *J* = 10.20 Hz, 2H, piperidine-H), 1.44−1.33 (m, 2H, piperidine-H). ¹³C NMR (75 MHz, DMSO-*d₆*, ppm) δ: 166.11, 160.08, 157.28, 153.99, 152.70, 145.94, 144.51, 136.16, 129.99, 129.49, 129.08, 128.80, 128.22, 79.20, 61.63, 51.97, 51.71, 47.21, 31.20, 20.29, 15.23. ESI-MS: *m/z* 501.4 (M+1), 523.5 (M+23), C₂₈H₃₂N₆O₃ (500.59).

*4.1.2.7. 7-(Mesityloxy)-N-(1-(4-nitrobenzyl)piperidin-4-yl)-[1,2,4] triazolo[1,5-a] pyrimidin-5-amine (**7g**).* Yellow solid, yield: 58%. mp: decomposed. ¹H NMR (300 MHz, DMSO-*d₆*, ppm) δ: 8.20 (s, 1H, triazole-H), 8.17 (d, *J* = 1.50 Hz, 2H, PhH), 7.59 (d, *J* = 8.70 Hz, 2H, PhH), 7.53 (d, *J* = 7.20 Hz, 1H, NH), 7.08 (s, 2H, OPh-H), 5.32 (s, 1H, pyrimidine-H), 3.84−3.82 (m, 1H, piperidine-H), 3.60 (s, 2H, CH₂), 2.73 (d, *J* = 11.70 Hz, 2H, piperidine-H), 2.30 (s, 3H, CH₃), 2.18−2.14 (m, 2H, piperidine-H), 2.09 (s, 6H, CH₃ ×2), 1.88 (d, *J* = 10.20 Hz, 2H, piperidine-H), 1.46−1.35 (m, 2H, piperidine-H). ¹³C NMR (75 MHz, DMSO-*d₆*, ppm) δ: 160.09, 157.28, 153.99, 152.71, 147.08, 146.50, 145.93, 136.17, 129.99, 129.55, 129.49, 123.31, 79.20, 61.13, 51.70, 47.15, 31.20, 20.29, 15.23. ESI-MS: *m/z* 488.5 (M+1), 510.5 (M+23), C₂₆H₂₉N₇O₃ (487.55).

*4.1.2.8. 4-((4-((7-(Mesityloxy)-[1,2,4]triazolo[1,5-a]pyrimidin-5-yl)amino)piperidin-1-yl)methyl)benzamide (**7h**).* White solid, yield: 32%. mp: decomposed. ¹H NMR (300 MHz, DMSO-*d₆*, ppm) δ: 8.17 (s, 1H, triazole-H), 7.90 (s, 1H, CONH₂), 7.82 (d, *J* = 8.40 Hz, 2H, PhH), 7.52 (d, *J* = 7.20 Hz, 1H, NH), 7.36 (d, *J* = 8.40 Hz, 2H, PhH), 7.28 (s, 1H, CONH₂), 7.08 (s, 2H, OPh-H), 5.31 (s, 1H, pyrimidine-H), 3.80 (m, 1H, piperidine-H), 3.50 (s, 2H, CH₂), 2.72 (d, *J* = 11.40 Hz, 2H, piperidine-H), 2.30 (s, 3H, CH₃), 2.13−2.09 (m, 8H, piperidine-H, CH₃), 1.86 (d, *J* = 9.60 Hz, 2H, piperidine-H), 1.43−1.32 (m, 2H, piperidine-H). ¹³C NMR (75 MHz, DMSO-*d₆*, ppm) δ: 167.74, 160.08, 157.28, 153.99, 152.69, 145.94, 142.01, 136.16, 132.95, 129.99, 129.50, 128.36, 127.37, 79.21, 61.70, 51.68, 47.25, 31.22, 20.29, 15.23. ESI-MS: *m/z* 486.5 (M+1), 487.5 (M+2), 488.5 (M+3), 508.4 (M+23), C₂₇H₃₁N₇O₂ (485.58).

*4.1.2.9. 1-(4-((4-((7-(Mesityloxy)-[1,2,4]triazolo[1,5-a]pyrimidin-5-yl)amino) piperidin-1-yl)methyl)phenyl)ethanone (**7i**).* White solid, yield: 43%. mp: >320 °C. ¹H NMR (300 MHz, DMSO-*d₆*, ppm) δ: 8.16 (s, 1H, triazole-H), 7.91 (d, *J* = 8.10 Hz, 2H, PhH), 7.52 (d, *J* = 7.20 Hz, 1H, NH), 7.44 (d, *J* = 8.10 Hz, 2H, PhH), 7.08 (s, 2H, OPh-H), 5.31 (s, 1H, pyrimidine-H), 3.80 (m, 1H, piperidine-H), 3.53 (s, 2H, CH₂), 2.72 (d, *J* = 11.10 Hz, 2H, piperidine-H), 2.56 (s, 3H, COCH₃), 2.30 (s, 3H, CH₃), 2.14−2.09 (m, 8H, piperidine-H, CH₃), 1.87 (d, *J* = 9.60 Hz, 2H, piperidine-H), 1.43−1.33 (m, 2H, piperidine-H). ¹³C NMR (75 MHz, DMSO-*d₆*, ppm) δ: 197.49, 160.08, 153.99, 152.70, 145.93, 144.34, 136.17, 135.63, 130.00, 129.49, 128.76, 128.16, 79.21, 61.65, 51.72, 47.21, 31.21, 26.63, 20.29, 15.24. ESI-MS: *m/z* 485.5 (M+1), 507.5 (M+23), C₂₈H₃₂N₆O₂ (484.59).

*4.1.2.10. N-(1-(4-bromobenzyl)piperidin-4-yl)-7-(mesityloxy)-[1,2,4] triazolo[1,5-a] pyrimidin-5-amine (**7j**).* White solid, yield: 42%.mp: 249.5−251.5 °C. ¹H NMR (300 MHz, DMSO-*d₆*, ppm) δ: 8.16 (s, 1H, triazole-H), 7.51−7.49 (m, 3H, NH, PhH), 7.25 (d, *J* = 8.10 Hz, 2H, PhH), 7.07 (s, 2H, OPh-H), 5.31 (s, 1H, pyrimidine-H), 3.80 (m, 1H, piperidine-H), 3.41 (s, 2H, CH₂), 2.71 (d, *J* = 11.40 Hz, 2H, piperidine-H), 2.30 (s, 3H, CH₃), 2.09 (m, 8H, piperidine-H, CH₃), 1.86 (d, *J* = 9.60 Hz, 2H, piperidine-H), 1.41−1.31 (m, 2H, piperidine-H). ¹³C NMR (75 MHz, DMSO-*d₆*, ppm) δ: 160.07, 157.27, 153.99, 152.69, 145.92, 136.17, 131.01, 130.83, 130.00, 129.49, 119.77, 79.19, 61.23, 51.59, 47.21, 31.20, 20.29, 15.24. ESI-MS: *m/z* 522.5 (M+1), 523.4 (M+2), C₂₆H₂₉BrN₆O (521.45).

*4.1.2.11. N-(1-(3-chlorobenzyl)piperidin-4-yl)-7-(mesityloxy)-[1,2,4] triazolo[1,5-a] pyrimidin-5-amine (**7k**).* White solid, yield: 39%. mp: 240−242.5 °C. ¹H NMR (300 MHz, DMSO-*d₆*, ppm) δ: 8.17 (s, 1H, triazole-H), 7.52 (d, *J* = 7.20 Hz, 1H, NH), 7.37−7.24 (m, 4H, PhH), 7.08 (s, 2H, OPh-H), 5.32 (s, 1H, pyrimidine-H), 3.82−3.80 (m, 1H, piperidine-H), 3.46 (s, 2H, CH₂), 2.72 (d, *J* = 11.40 Hz, 2H, piperidine-H), 2.30 (s, 3H, CH₃), 2.13−2.09 (m, 8H, piperidine-H, CH₃), 1.87 (d, *J* = 10.20 Hz, 2H, piperidine-H), 1.42−1.32 (m, 2H, piperidine-H). ¹³C NMR (75 MHz, DMSO-*d₆*, ppm) δ: 160.09, 157.28, 153.99, 152.70, 145.94, 141.37, 136.16, 132.87, 129.99, 129.49, 128.26, 127.26, 126.77, 79.21, 61.29, 51.60, 47.22, 31.20, 20.29, 15.23. ESI-MS: *m/z* 477.4 (M), 499.5 (M+22), C₂₆H₂₉ClN₆O (477.00).

*4.1.2.12. 4-((4-((7-(Mesityloxy)-[1,2,4]triazolo[1,5-a]pyrimidin-5-yl) amino)piperidin-1-yl)methyl)benzonitrile (**7l**).* White solid, yield: 61%. mp: 250−251 °C. ¹H NMR (300 MHz, DMSO-*d₆*, ppm) δ: 8.17 (s, 1H, triazole-H), 7.78 (d, *J* = 8.40 Hz, 2H, PhH), 7.53 (d, *J* = 6.60 Hz, 1H, NH), 7.50 (d, *J* = 8.10 Hz, 2H, PhH), 7.08 (s, 2H, OPh-H), 5.32 (s, 1H, pyrimidine-H), 3.83−3.81 (m, 1H, piperidine-H), 3.55 (s, 2H, CH₂), 2.71 (d, *J* = 11.70 Hz, 2H, piperidine-H), 2.30 (s, 3H, CH₃), 2.16−2.12 (m, 2H, piperidine-H), 2.09 (s, 6H, CH₃ ×2), 1.87 (d, *J* = 10.20 Hz, 2H, piperidine-H), 1.44−1.33 (m, 2H, piperidine-H). ¹³C NMR (75 MHz, DMSO-*d₆*, ppm) δ: 160.09, 157.28, 153.99, 152.71, 145.94, 144.81, 136.16, 132.10, 129.99, 129.49, 129.40, 118.86, 109.59, 79.20, 61.44, 51.67, 47.16, 31.20, 20.28, 15.23. ESI-MS: *m/z* 468.4 (M+1), 490.6 (M+23), C₂₇H₂₉N₇O (467.57).

*4.1.2.13. 3-((4-((7-(Mesityloxy)-[1,2,4]triazolo[1,5-a]pyrimidin-5-yl) amino)piperidin-1-yl)methyl)benzonitrile (**7m**).* White solid, yield: 55%. mp: decomposed. ¹H NMR (300 MHz, DMSO-*d₆*, ppm) δ: 8.17 (s, 1H, triazole-H), 7.72−7.70 (m, 2H, PhH), 7.65 (d, *J* = 7.80 Hz, 1H, NH), 7.56−7.51 (m, 2H, PhH), 7.08 (s, 2H, OPh-H), 5.32 (s, 1H, pyrimidine-H), 3.83−3.81 (m, 1H, piperidine-H), 3.52 (s, 2H, CH₂), 2.72 (d, *J* = 11.40 Hz, 2H, piperidine-H), 2.30 (s, 3H, CH₃), 2.15 (m, 2H, piperidine-H), 2.09 (s, 6H, CH₃ ×2), 1.87 (d, *J* = 10.20 Hz, 2H, piperidine-H), 1.43−1.33 (m, 2H, piperidine-H). ¹³C NMR (75 MHz, DMSO-*d₆*, ppm) δ: 160.09, 157.28, 153.99, 152.70, 145.94, 140.44, 136.16, 133.54, 131.97, 130.70, 129.99, 129.49, 129.40, 118.84, 111.17, 79.20, 60.97, 51.56, 47.18, 31.18, 20.29, 15.23. ESI-MS: *m/z* 468.4 (M+1), 490.6 (M+23), C₂₇H₂₉N₇O (467.57).

*4.1.2.14. 2-((4-((7-(Mesityloxy)-[1,2,4]triazolo[1,5-a]pyrimidin-5-yl) amino)piperidin-1-yl)methyl)benzonitrile (**7n**).* White solid, yield: 57%. mp: 252.5−253.5 °C. ¹H NMR (300 MHz, DMSO-*d₆*, ppm) δ: 8.17 (s, 1H, triazole-H), 7.80 (dd, *J* = 7.50 Hz, *J* = 0.90 Hz, 1H, PhH), 7.67 (td, *J* = 7.50 Hz, *J* = 1.20 Hz, 1H, PhH), 7.56 (d, *J* = 7.80 Hz, 1H, PhH), 7.53 (d, *J* = 7.50 Hz, 1H, NH), 7.46 (td, *J* = 7.50 Hz, *J* = 0.90 Hz, 1H, PhH), 7.08 (s, 2H, OPh-H), 5.32 (s, 1H, pyrimidine-H), 3.85−3.84 (m, 1H, piperidine-H), 3.63 (s, 2H, CH₂), 2.73 (d, *J* = 11.70 Hz, 2H, piperidine-H), 2.30 (s, 3H, CH₃), 2.24−2.18 (m, 2H, piperidine-H), 2.09 (s, 6H, CH₃ ×2), 1.87 (d, *J* = 9.90 Hz, 2H, piperidine-H), 1.44−1.32 (m, 2H, piperidine-H). ¹³C NMR (75 MHz, DMSO-*d₆*,

ppm) δ: 160.09, 157.28, 153.99, 152.70, 145.94, 142.40, 136.16, 132.95, 132.93, 129.99, 129.49, 127.86, 117.62, 112.01, 79.22, 59.85, 51.53, 47.04, 31.08, 20.28, 15.23. ESI-MS: m/z 468.4 (M+1), 469.5 (M+2), 470.6 (M+3), 490.6 (M+23), $C_{27}H_{29}N_7O$ (467.57).

4.1.2.15. N-(1-(4-fluorobenzyl)piperidin-4-yl)-7-(mesityloxy)-[1,2,4] triazolo[1,5-a] pyrimidin-5-amine (7o). White solid, yield: 54%. mp: 249–249.5 °C. ^{1}H NMR (300 MHz, DMSO-d_6, ppm) δ: 8.17 (s, 1H, triazole-H), 7.52 (d, J = 7.20 Hz, 1H, NH), 7.32 (dd, J_{H-H} = 8.40 Hz, J_{H-F} = 5.70 Hz, 2H, PhH), 7.12 (dd, J_{H-H} = 6.90 Hz, J_{H-F} = 8.90 Hz, 2H, PhH), 7.07 (s, 2H, OPh-H), 5.31 (s, 1H, pyrimidine-H), 3.82–3.78 (m, 1H, piperidine-H), 3.43 (s, 2H, CH_2), 2.71 (d, J = 11.70 Hz, 2H, piperidine-H), 2.30 (s, 3H, CH_3), 2.09–2.04 (m, 8H, piperidine-H, CH_3), 1.86 (d, J = 9.90 Hz, 2H, piperidine-H), 1.42–1.30 (m, 2H, piperidine-H). ^{13}C NMR (75 MHz, DMSO-d_6, ppm) δ: 161.16 (d, J_{C-F} = 239.25 Hz, 1C, Ph-C), 160.08, 157.28, 153.98, 152.69, 145.94, 136.16, 134.71 (d, J_{C-F} = 3.00 Hz, 1C, Ph-C), 130.47 (d, J_{C-F} = 7.50 Hz, 2C, Ph-C), 129.99, 129.49, 114.79 (d, J_{C-F} = 21.00 Hz, 2C, Ph-C), 79.20, 61.20, 51.55, 47.30, 31.21, 20.28, 15.23. ESI-MS: m/z 461.4 (M+1), 483.4 (M+23), $C_{26}H_{29}FN_6O$ (460.55).

4.1.2.16. N-(1-(3-fluorobenzyl)piperidin-4-yl)-7-(mesityloxy)-[1,2,4] triazolo[1,5-a] pyrimidin-5-amine (7p). White solid, yield: 52%. mp: 246.5–247 °C. ^{1}H NMR (300 MHz, DMSO-d_6, ppm) δ: 8.17 (s, 1H, triazole-H), 7.52 (d, J = 7.20 Hz, 1H, NH), 7.39–7.32 (m, 1H, PhH), 7.15–7.04 (m, 5H, PhH, OPh-H), 5.32 (s, 1H, pyrimidine-H), 3.81 (m, 1H, piperidine-H), 3.47 (s, 2H, CH_2), 2.73 (d, J = 10.80 Hz, 2H, piperidine-H), 2.30 (s, 3H, CH_3), 2.13–2.09 (m, 8H, piperidine-H, CH_3), 1.87 (d, J = 10.50 Hz, 2H, piperidine-H), 1.43–1.33 (m, 2H, piperidine-H). ^{13}C NMR (75 MHz, DMSO-d_6, ppm) δ: 162.20 (d, J_{C-F} = 242.25 Hz, 1C, Ph-C), 160.09, 157.28, 153.99, 152.70, 145.94, 141.84, 136.16, 129.99, 129.49, 124.54, 115.01 (d, J_{C-F} = 21.00 Hz, 2C, Ph-C), 113.54 (d, J_{C-F} = 20.25 Hz, 2C, Ph-C), 79.21, 61.37, 51.62, 47.23, 31.21, 20.28, 15.23. ESI-MS: m/z 461.4 (M+1), $C_{26}H_{29}FN_6O$ (460.55).

4.1.2.17. N-(1-(2-fluorobenzyl)piperidin-4-yl)-7-(mesityloxy)-[1,2,4] triazolo[1,5-a] pyrimidin-5-amine (7q). White solid, yield: 56%. mp: 248.5–251.5 °C. ^{1}H NMR (300 MHz, DMSO-d_6, ppm) δ: 8.16 (s, 1H, triazole-H), 7.51 (d, J = 7.20 Hz, 1H, NH), 7.39 (ddd, J_{H-H} = 7.50 Hz, J_{H-F} = 5.70 Hz, J_{H-H} = 1.50 Hz, 1H, PhH), 7.35–7.27 (m, 1H, PhH), 7.19–7.12 (m, 2H, PhH), 7.07 (s, 2H, OPh-H), 5.31 (s, 1H, pyrimidine-H), 3.81–3.79 (m, 1H, piperidine-H), 3.50 (s, 2H, CH_2), 2.74 (d, J = 11.70 Hz, 2H, piperidine-H), 2.30 (s, 3H, CH_3), 2.16–2.09 (m, 8H, piperidine-H, CH_3), 1.86 (d, J = 9.90 Hz, 2H, piperidine-H), 1.42–1.30 (m, 2H, piperidine-H). ^{13}C NMR (75 MHz, DMSO-d_6, ppm) δ: 160.72 (d, J_{C-F} = 243.00 Hz, 1C, Ph-C), 160.07, 157.27, 153.99, 152.69, 145.93, 136.16, 131.44 (d, J_{C-F} = 4.50 Hz, 1C, Ph-C), 129.99, 129.49, 128.92 (d, J_{C-F} = 7.50 Hz, 1C, Ph-C), 124.86 (d, J_{C-F} = 14.25 Hz, 1C, Ph-C), 124.11 (d, J_{C-F} = 3.00 Hz, 1C, Ph-C), 115.07 (d, J_{C-F} = 22.50 Hz, 1C, Ph-C), 79.19, 54.61, 51.49, 47.15, 31.16, 20.29, 15.23. ESI-MS: m/z 461.4 (M+1), $C_{26}H_{29}FN_6O$ (460.55).

4.1.2.18. 7-(Mesityloxy)-N-(1-(4-methylbenzyl)piperidin-4-yl)-[1,2,4] triazolo[1,5-a] pyrimidin-5-amine (7r). White solid, yield: 65%. mp: 249.5–250.5 °C. ^{1}H NMR (300 MHz, DMSO-d_6, ppm) δ: 8.16 (s, 1H, triazole-H), 7.51 (d, J = 7.20 Hz, 1H, NH), 7.17–7.09 (m, 4H, PhH), 7.07 (s, 2H, OPh-H), 5.31 (s, 1H, pyrimidine-H), 3.81–3.79 (m, 1H, piperidine-H), 3.39 (s, 2H, CH_2), 2.71 (d, J = 11.40 Hz, 2H, piperidine-H), 2.30 (s, 3H, CH_3), 2.27 (s, 3H, CH_3), 2.09–1.99 (m, 8H, piperidine-H, CH_3), 1.85 (d, J = 12.30 Hz, 2H, piperidine-H), 1.40–1.30 (m, 2H, piperidine-H). ^{13}C NMR (75 MHz, DMSO-d_6, ppm) δ: 160.08, 157.28, 153.98, 152.69, 145.94, 136.15, 135.79, 135.45, 129.99, 129.49, 128.66, 79.19, 61.91, 51.59, 47.33, 31.22, 20.63, 20.29, 15.23. ESI-MS: m/z 457.5 (M+1), 479.4 (M+23), $C_{27}H_{32}N_6O$ (456.58).

4.1.2.19. 7-(Mesityloxy)-N-(1-(2-methylbenzyl)piperidin-4-yl)-[1,2,4] triazolo[1,5-a] pyrimidin-5-amine (7s). White solid, yield: 67%. mp: 255–257.5 °C. ^{1}H NMR (300 MHz, DMSO-d_6, ppm) δ: 8.16 (s, 1H, triazole-H), 7.50 (d, J = 7.50 Hz, 1H, NH), 7.48 (d, J = 8.10 Hz, 2H, PhH), 7.21–7.19 (m, 1H, PhH), 7.14–7.10 (m, 3H, PhH), 7.07 (s, 2H, OPh-H), 5.31 (s, 1H, pyrimidine-H), 3.83–3.78 (m, 1H, piperidine-H), 3.40 (s, 2H, CH_2), 2.72 (d, J = 11.70 Hz, 2H, piperidine-H), 2.30 (s, 3H, CH_3), 2.29 (s, 3H, CH_3), 2.14–2.09 (m, 8H, piperidine-H, CH_3), 1.87 (d, J = 10.50 Hz, 2H, piperidine-H), 1.39–1.28 (m, 2H, piperidine-H). ^{13}C NMR (75 MHz, DMSO-d_6, ppm) δ: 160.08, 157.28, 153.98, 152.68, 145.93, 136.91, 136.62, 136.16, 129.99, 129.49, 129.40, 126.77, 125.34, 79.20, 60.16, 51.79, 47.35, 31.30, 20.29, 18.75, 15.23. ESI-MS: m/z 457.6 (M+1), 479.5 (M+23), $C_{27}H_{32}N_6O$ (456.58).

4.1.2.20. N-(1-(2,4-difluorobenzyl)piperidin-4-yl)-7-(mesityloxy)-[1,2,4]triazolo[1,5-a] pyrimidin-5-amine (7t). White solid, yield: 64%. mp: 249–249.5 °C. ^{1}H NMR (300 MHz, DMSO-d_6, ppm) δ: 8.17 (s, 1H, triazole-H), 7.51 (d, J = 7.20 Hz, 1H, NH), 7.43 (dd, J_{H-F} = 15.30 Hz, J_{H-H} = 8.40 Hz, 1H, PhH), 7.18 (td, J_{H-F} = 9.90 Hz, J_{H-H} = 2.40 Hz, 2H, PhH), 7.07–7.04 (m, 3H, OPh-H, PhH), 5.31 (s, 1H, pyrimidine-H), 3.81–3.79 (m, 1H, piperidine-H), 3.48 (s, 2H, CH_2), 2.72 (d, J = 11.70 Hz, 2H, piperidine-H), 2.29 (s, 3H, CH_3), 2.15–2.09 (m, 8H, piperidine-H, CH_3), 1.86 (d, J = 10.20 Hz, 2H, piperidine-H), 1.42–1.29 (m, 2H, piperidine-H). ^{13}C NMR (75 MHz, DMSO-d_6, ppm) δ: 163.05, 162.21, 160.08, 158.93, 157.28, 153.98, 152.70, 145.93, 136.16, 132.64, 132.56, 132.43, 129.98, 129.49, 121.33, 121.28, 121.13, 121.08, 111.30, 111.25, 111.02, 103.86, 103.51, 103.16, 79.20, 54.11, 51.35, 47.13, 31.14, 20.28, 15.22. ESI-MS: m/z 479.4 (M+1), 501.4 (M+23), $C_{26}H_{28}F_2N_6O$ (478.54).

4.1.2.21. N-(1-(3,4-difluorobenzyl)piperidin-4-yl)-7-(mesityloxy)-[1,2,4]triazolo[1,5-a] pyrimidin-5-amine (7u). White solid, yield: 48%. mp: 253–256 °C. ^{1}H NMR (300 MHz, DMSO-d_6, ppm) δ: 8.17 (s, 1H, triazole-H), 7.52 (d, J = 7.20 Hz, 1H, NH), 7.40–7.29 (m, 2H, PhH), 7.15–7.11 (m, 1H, PhH), 7.08 (s, 2H, OPh-H), 5.32 (s, 1H, pyrimidine-H), 3.82–3.80 (m, 1H, piperidine-H), 3.44 (s, 2H, CH_2), 2.72 (d, J = 11.70 Hz, 2H, piperidine-H), 2.30 (s, 3H, CH_3), 2.13–2.06 (m, 8H, piperidine-H, CH_3), 1.87 (d, J = 10.20 Hz, 2H, piperidine-H), 1.42–1.32 (m, 2H, piperidine-H). ^{13}C NMR (75 MHz, DMSO-d_6, ppm) δ: 160.08, 157.27, 153.98, 152.69, 145.93, 136.62, 136.58, 136.56, 136.51, 136.16, 129.99, 129.49, 125.17, 125.13, 125.08, 125.04, 117.31, 117.12, 116.90, 79.20, 60.73, 51.51, 47.22, 31.19, 20.28, 15.23. ESI-MS: m/z 479.4 (M+1), 501.4 (M+23), $C_{26}H_{28}F_2N_6O$ (478.54).

4.1.2.22. N-(1-(2,5-difluorobenzyl)piperidin-4-yl)-7-(mesityloxy)-[1,2,4]triazolo[1,5-a] pyrimidin-5-amine (7v). White solid, yield: 63%. mp: 244.5–245 °C. ^{1}H NMR (300 MHz, DMSO-d_6, ppm) δ: 8.17 (s, 1H, triazole-H), 7.52 (d, J = 7.20 Hz, 1H, NH), 7.26–7.20 (m, 2H, PhH), 7.18–7.10 (m, 1H, PhH), 7.07 (s, 2H, OPh-H), 5.32 (s, 1H, pyrimidine-H), 3.82–3.80 (m, 1H, piperidine-H), 3.51 (s, 2H, CH_2), 2.74 (d, J = 11.40 Hz, 2H, piperidine-H), 2.30 (s, 3H, CH_3), 2.19–2.09 (m, 8H, piperidine-H, CH_3), 1.87 (d, J = 10.20 Hz, 2H, piperidine-H), 1.44–1.33 (m, 2H, piperidine-H). ^{13}C NMR (75 MHz, DMSO-d_6, ppm) δ: 160.09, 159.61, 158.34, 157.28, 156.46, 155.16, 153.98, 152.70, 145.93, 136.15, 129.98, 129.49, 127.35, 127.25, 127.12, 127.02, 117.27, 117.20, 116.95, 116.88, 116.79, 116.68, 116.46, 116.34, 115.38, 115.26, 115.06, 114.94, 79.21, 54.23, 51.45, 47.07, 31.15, 20.27, 15.22. ESI-MS: m/z 479.4 (M+1), 501.4 (M+23), $C_{26}H_{28}F_2N_6O$ (478.54).

4.1.2.23. N-(1-(2,6-difluorobenzyl)piperidin-4-yl)-7-(mesityloxy)-[1,2,4]triazolo[1,5-a] pyrimidin-5-amine (7w). White solid, yield: 51%. mp: 254.5–256 °C. ^{1}H NMR (300 MHz, DMSO-d_6, ppm) δ: 8.16 (s, 1H, triazole-H), 7.49 (d, J = 7.20 Hz, 1H, NH), 7.45–7.35 (m, 1H, PhH), 7.12–7.07 (m, 4H, PhH, OPh-H), 5.30 (s, 1H, pyrimidine-H), 3.78–3.76 (m, 1H, piperidine-H), 3.55 (s, 2H, CH_2), 2.73 (d,

$J = 11.70$ Hz, 2H, piperidine-H), 2.29 (s, 3H, CH_3), 2.18–2.08 (m, 8H, piperidine-H, CH_3), 1.84 (d, $J = 10.20$ Hz, 2H, piperidine-H), 1.39–1.27 (m, 2H, piperidine-H). ^{13}C NMR (75 MHz, DMSO-d_6, ppm) δ: 161.35 (dd, $J_{C-F} = 245.25$ Hz, $J_{C-F} = 8.25$ Hz, 2C, Ph-C), 160.06, 157.27, 153.98, 152.69, 145.92, 136.15, 129.98, 129.91 (t, $J_{C-F} = 10.50$ Hz, 1C, Ph-C), 129.49, 113.03 (t, $J_{C-F} = 19.50$ Hz, 1C, Ph-C), 111.33 (d, $J_{C-F} = 25.50$ Hz, 2C, Ph-C), 79.19, 51.13, 48.35, 46.96, 31.07, 20.27, 15.22. ESI-MS: m/z 479.4 (M+1), 501.4 (M+23), $C_{26}H_{28}F_2N_6O$ (478.54).

*4.1.2.24. Methyl-3-chloro-4-(2-(4-((7-(mesityloxy)-[1,2,4]triazolo[1,5-a]pyrimidin-5-yl)amino)piperidin-1-yl)acetamido)benzoate (**8a**).* White solid, yield: 61%. mp: 262.5–264 °C. ^{1}H NMR (400 MHz, DMSO-d_6, ppm) δ: 10.33 (s, 1H, CONH), 8.52 (d, $J = 8.64$ Hz, 1H, PhH), 8.18 (s, 1H, triazole-H), 8.02 (d, $J = 1.88$ Hz, 1H, PhH), 7.95 (dd, $J = 8.64$ Hz, $J = 1.80$ Hz, 1H, PhH), 7.57 (d, $J = 7.28$ Hz, 1H, NH), 7.09 (s, 2H, OPh-H), 5.30 (s, 1H, pyrimidine-H), 3.89 (m, 1H, piperidine-H), 3.85 (s, 3H, $COOCH_3$), 3.23 (s, 2H, CH_2), 2.87 (d, $J = 11.56$ Hz, 2H, piperidine-H), 2.47–2.41 (m, 2H, piperidine-H), 2.31 (s, 3H, CH_3), 2.10 (s, 6H, $CH_3 \times 2$), 1.96 (d, $J = 10.76$ Hz, 2H, piperidine-H), 1.55–1.50 (m, 2H, piperidine-H). ^{13}C NMR (100 MHz, DMSO-d_6, ppm) δ: 169.69, 165.19, 160.58, 157.79, 154.53, 153.26, 146.44, 138.95, 136.70, 130.50, 130.40, 130.00, 129.77, 125.78, 122.23, 120.02, 79.73, 61.73, 52.77, 52.34, 46.89, 32.12, 20.80, 15.75. ESI-MS: m/z 578.5 (M), 580.4 (M+2), 600.5 (M+22), $C_{29}H_{32}ClN_7O_4$ (578.06).

*4.1.2.25. 3-Bromo-4-(2-(4-((7-(mesityloxy)-[1,2,4]triazolo[1,5-a]pyrimidin-5-yl)amino) piperidin-1-yl)acetamido)benzoic acid (**8b**).* White solid, yield: 25%. mp: >320 °C. ^{1}H NMR (300 MHz, DMSO-d_6, ppm) δ: 13.00 (brs, 1H, COOH), 10.31 (s, 1H, CONH), 8.50 (d, $J = 8.40$ Hz, 1H, PhH), 8.18 (s, 1H, triazole-H), 8.14 (d, $J = 1.80$ Hz, 1H, PhH), 7.95 (dd, $J = 8.70$ Hz, $J = 1.50$ Hz, 1H, PhH), 7.54 (d, $J = 7.20$ Hz, 1H, NH), 7.09 (s, 2H, OPh-H), 5.30 (s, 1H, pyrimidine-H), 3.91–3.85 (m, 1H, piperidine-H), 3.21 (s, 2H, CH_2), 2.87 (d, $J = 11.70$ Hz, 2H, piperidine-H), 2.45–2.42 (m, 2H, piperidine-H), 2.30 (s, 3H, CH_3), 2.10 (s, 6H, $CH_3 \times 2$), 1.96 (d, $J = 10.20$ Hz, 2H, piperidine-H), 1.63–1.53 (m, 2H, piperidine-H). ^{13}C NMR (75 MHz, DMSO-d_6, ppm) δ: 169.23, 165.63, 160.06, 157.29, 154.03, 152.76, 145.92, 139.21, 136.20, 133.26, 130.01, 129.89, 129.50, 119.36, 111.84, 79.20, 61.28, 51.86, 31.52, 20.30, 15.25. ESI-MS: m/z 608.3 (M), 630.4 (M+22), $C_{28}H_{30}BrN_7O_4$ (608.49).

4.2. In vitro anti-HIV assay

Evaluation of the antiviral activity and cytotoxicity of the synthesized compounds was performed using the MTT assay as previously described [27,28]. Stock solutions (10× final concentration) of test compounds were added in 25 μL volumes to two series of triplicate wells to allow simultaneous evaluation of their effects on mock- and HIV-infected cells at the beginning of each experiment. Serial five-fold dilutions of test compounds were made directly in flat-bottomed 96-well microtiter trays by adding 100 μL medium to the 25 μL stock solution and transferring 25-μL of this solution to another well that contained 100 μL medium using a Biomek 3000 robot (Beckman instruments, Fullerton, CA). Untreated control HIV- and mock-infected cell samples were included for each sample. HIV-1 wt strain (IIIB), HIV-1 double mutant strain (RES056) or HIV-2 strain (ROD) stock (50 μL) at 100–300 CCID50 (50% cell culture infectious dose) or culture medium was added to either the infected or mock-infected wells of the microtiter tray. Mock-infected cells were used to evaluate the effect of test compounds on uninfected cells in order to assess its cytotoxicity. Exponentially growing MT-4 cells were centrifuged for 5 min at 1000 rpm and the supernatant was discarded. The MT-4 cells were resuspended at 6×10^5 cells/ mL, and 50 μL volumes were transferred to the microtiter tray wells. Five days after infection, the viability of mock- and HIV-infected cells was examined spectrophotometrically by the MTT method. The 50% cytotoxic concentration (CC_{50}) was defined as the concentration of the test compound that reduced the viability of the mock-infected MT-4 cells by 50%. The concentration achieving 50% protection from the cytopathic effect of the virus in infected cells was defined as the 50% effective concentration (EC_{50}).

4.3. HIV-1 RT inhibition assay

The inhibition assay of HIV-1 RT_{wt} was performed by utilizing the template/primer hybrid poly(A) × oligo(dT)$_{15}$, digoxigenin- and biotin-labeled nucleotides, an antibody to digoxigenin which was conjugated to peroxidase (anti-DIG-POD), and the peroxidase substrate ABTS. The incorporation quantities of the digoxigenin- and biotin-labeled dUTP into DNA represented the activity of HIV-1 RT. The HIV-RT inhibition assay was implemented by using an RT assay kit (Roche), and the procedures for assaying RT inhibition was done as described in the kit protocol [29,30]. The tested compound **7d** and two control drugs NVP and ETR was used at different concentration gradient (1.040, 0.208, 0.0416, 0.00832, 0.001664 μM for **7d**; 100, 20, 4, 0.8, 0.16 μM for NVP; 1, 0.2, 0.04, 0.008, 0.0016 μM for ETR). Concretely, the reaction mixture consisted of template/primer complex, 2′-deoxy-nucleotide-5′-triphosphates (dNTPs) and RT enzyme in the lysis buffer with or without inhibitors. After incubation for 1 h at 37 °C, the reaction mixture was transferred to streptavidin-coated microtiter plate (MTP). The biotin labeled dNTPs that are incorporated in the template due to presence of RT were bound to streptavidine. The unbound dNTPs were washed using wash buffer and then antidigoxigenin-peroxidase (anti-DIG-POD) was added in MTP. The DIG-labeled dNTPs incorporated in the template was bound to anti-DIG-POD antibody. The unbound anti-DIG-POD was also washed elaborately for 5 times by using wash buffer and finally, the peroxide substrate (ABST) was added to the MTP. A colored reaction product emerged during the cleavage of the substrate catalyzed by a peroxide enzyme. The absorbance of the sample was determined at OD_{450} using microtiter plate ELISA reader. The percentage inhibitory activity of RT inhibitors was calculated by comparison with a sample lacking an inhibitor. The resulting color intensity is directly proportional to RT activity. The percentage inhibitory values were calculated by the following formula: %Inhibition = [O.D. value without inhibitors (with RT) − O.D.value with RT and inhibitors]/[O.D. value with RT and inhibitors-O.D. value without RT and inhibitors]. The IC_{50} value corresponded to the concentration of the tested compound required to inhibit the incorporation of the labeled dUTP into RT by 50%.

4.4. Molecular simulations

The molecules (**7d** and the lead compound **LW-7c**) for docking were optimized for 2000-generations until the maximum derivative of energy became 0.005 kcal/(mol*Å), using the Tripos force field. Charges were computed and added according to Gasteiger−Huckel parameters. The published 3D crystal structures of wt RT complexes (PDB code: 3M8Q [19]) was retrieved from the Protein Data Bank [23] and was used for the docking studies by means of surflex-dock module of SYBYL-X 1.1 [24]. The protein was prepared by using the Biopolymer application accompanying SYBYL according to SYBYL-X 1.1 manual: The bound ligand was extracted from the complexes, water molecules were removed, hydrogen atoms were automatically added (after which the resulting structures haven't been optimized), and charges and atom types were assigned according to AMBER99. After the protomol was generated,

which referred to a computational representation of the intended binding site to which putative ligands are aligned, the optimized compounds **7d** and **LW-7c** were docked into NNIBP, with the relevant parameters set as defaults. The original ligand of the co-ordinates (3M8Q) was used as reference molecule to calculate the RMSD values. The docking scores related to binding affinities were calculated based on hydrophobic, polar, and repulsive interactions as well as entropic effects and solvation. Top-scoring poses of compounds were shown by the software of PyMOL version 1.5 (http://www.pymol.org/). The secondary structure of RT was shown in cartoons, and only the key residues for interactions with the inhibitors were labeled and shown in sticks. The potential hydrogen bonds were presented by dashed lines.

4.5. Measurements of water solubility and log P of **7d**

4.5.1. Water solubility measurements

Water solubility was measured at pH 7 by using an HPLC-UV method [8a]. **7d** was initially dissolved in DMSO at 10 mg/mL. 10 μL of this stock solution was spiked into purified water (1 mL) with the final DMSO concentration being 1%. The mixture was shaked for 2 h with an IKA® MS3 digital micro-shaker at 3000 rpm at room temperature and left to sit for 1 h. The saturated solution was filtrated through a filter membrane (pore size = 0.22 μm) and transferred to other eppendorf tubes for analysis by HPLC–UV. The sample was performed in duplicate. For quantification, a model LC-20AT HPLC–UV (SHIMADZU) system was used with an Inertsil® ODS-SP-C18 column (150 mm × 4.6 mm, 5 μm) and eluant is MeOH/water (85/15). The flow rate was 1.0 mL/min, and injection volume was 10 μL. Aqueous concentration was determined by comparison of the peak area of the saturated solution with a standard curve plotted peak area versus known concentrations, which were prepared by solutions of compound **7d** in MeOH at 100, 25, 6.25, 1.56, and 0.39 μg/mL.

4.5.2. log P measurements

DMSO stock solution of **7d** (1 mg/mL) was prepared, and then 20 μL of this solution was added into *n*-octanol (1 mL) and H_2O (1 mL). The mixture was shaked for 2 h with the IKA® MS3 digital micro-shaker at 3000 rpm at room temperature and left to sit overnight. Each solution (~0.4 mL) was transferred from two phases, respectively, into other eppendorf tubes for HPLC analysis. The instrument and conditions were the same as those for solubility determination. The P (partition coefficient) value was calculated by the peak area ratios in *n*-octanol and in H_2O.

Conflict of interest

The authors declare no conflict of interest.

Acknowledgment

Appendix A. Supplementary data

Supplementary data related to this article can be found at http://dx.doi.org/10.1016/j.ejmech.2015.01.042.

References

[1] E.L. Asahchop, M.A. Wainberg, R.D. Sloan, C.L. Tremblay, Antiviral drug resistance and the need for development of new HIV-1 reverse transcriptase inhibitors, Antimicrob. Agents. Chemother. 56 (2012) 5000–5008.

[2] P. Zhan, X. Chen, D. Li, Z. Fang, E. De Clercq, X. Liu, HIV-1 NNRTIs: structural diversity, pharmacophore similarity, and implications for drug design, Med. Res. Rev. 33 (2013) E1–E72.

[3] D. Li, P. Zhan, E. De Clercq, X. Liu, Strategies for the design of HIV-1 non-nucleoside reverse transcriptase inhibitors: lessons from the development of seven representative paradigms, J. Med. Chem. 55 (2012) 3595–3613.

[4] (a) P. Zhan, X. Liu, Z. Li, Recent advances in the discovery and development of novel HIV-1 NNRTI platforms: 2006-2008 update, Curr. Med. Chem. 16 (2009) 2876–2889;
(b) Y. Song, Z. Fang, P. Zhan, X. Liu, Recent advances in the discovery and development of novel HIV-1 NNRTI platforms (part II): 2009–2013 update, Curr. Med. Chem. 21 (2013) 329–355.

[5] (a) P. Zhan, X. Liu, Novel HIV-1 non-nucleoside reverse transcriptase inhibitors: a patent review (2005–2010), Expert Opin. Ther. Pat. 21 (2011) 717–796;
(b) X. Li, L. Zhang, Y. Tian, Y. Song, P. Zhan, X. Liu, Novel HIV-1 non-nucleoside reverse transcriptase inhibitors: a patent review (2011–2014), Expert Opin. Ther. Pat. 24 (2014) 1199–1227.

[6] P. Zhan, X. Liu, Z. Li, C. Pannecouque, E. De Clercq, Design strategies of novel NNRTIs to overcome drug resistance, Curr. Med. Chem. 16 (2009) 3903–3917.

[7] X. Chen, P. Zhan, D. Li, X. Liu, E. De Clercq, Recent advances in DAPYs and related analogues as HIV-1 NNRTIs, Curr. Med. Chem. 18 (2011) 359–376.

[8] (a) L.Q. Sun, L. Zhu, K. Qian, B. Qin, L. Huang, C.H. Chen, K.H. Lee, L. Xie, Design, synthesis, and preclinical evaluations of novel 4-substituted 1,5-diarylanilines as potent HIV-1 non-nucleoside reverse transcriptase inhibitor (NNRTI) drug candidates, J. Med. Chem. 55 (2012) 7219–7229;
(b) B. Qin, X. Jiang, H. Lu, X. Tian, F. Barbault, L. Huang, K. Qian, C.H. Chen, R. Huang, S. Jiang, K.H. Lee, L. Xie, Diarylaniline derivatives as a distinct class of HIV-1 non-nucleoside reverse transcriptase inhibitors, J. Med. Chem. 53 (2010) 4906–4916;
(c) X. Tian, B. Qin, Z. Wu, X. Wang, H. Lu, S.L. Morris-Natschke, C.H. Chen, S. Jiang, K.H. Lee, L. Xie, Design, synthesis, and evaluation of diarylpyridines and diarylanilines as potent non-nucleoside HIV-1 reverse transcriptase inhibitors, J. Med. Chem. 53 (2010) 8287–8297;
(d) G. Meng, Y. Liu, A. Zheng, F. Chen, W. Chen, E. De Clercq, C. Pannecouque, J. Balzarini, Design and synthesis of a new series of modified CH-diarylpyrimidines as drug-resistant HIV non-nucleoside reverse transcriptase inhibitors, Eur. J. Med. Chem. 82 (2014) 600–611.

[9] D. Li, P. Zhan, H. Liu, C. Pannecouque, J. Balzarini, E. De Clercq, X. Liu, Synthesis and biological evaluation of pyridazine derivatives as novel HIV-1 NNRTIs, Bioorg. Med. Chem. 21 (2013) 2128–2134.

[10] J. Wang, P. Zhan, Z. Li, H. Liu, E. De Clercq, C. Pannecouque, X. Liu, Discovery of nitropyridine derivatives as potent HIV-1 non-nucleoside reverse transcriptase inhibitors via a structure-based core refining approach, Eur. J. Med. Chem. 76 (2014) 531–538.

[11] X. Li, W. Chen, Y. Tian, H. Liu, P. Zhan, E. De Clercq, C. Pannecouque, J. Balzarini, X. Liu, Discovery of novel diarylpyrimidines as potent HIV NNRTIs via a structure-guided core-refining approach, Eur. J. Med. Chem. 80 (2014) 112–121.

[12] X. Chen, P. Zhan, X. Liu, Z. Cheng, C. Meng, S. Shao, C. Pannecouque, E. De Clercq, X. Liu, Design, synthesis, anti-HIV evaluation and molecular modeling of piperidine-linked amino-triazine derivatives as potent non-nucleoside reverse transcriptase inhibitors, Bioorg. Med. Chem. 20 (2012) 3856–3864.

[13] X. Chen, Y. Li, S. Ding, J. Balzarini, C. Pannecouque, E. De Clercq, H. Liu, X. Liu, Discovery of piperidine-linked pyridine analogues as potent non-nucleoside HIV-1 reverse transcriptase inhibitors, ChemMedChem 8 (2013) 1117–1126.

[14] L. Zhang, P. Zhan, X. Chen, Z. Li, Z. Xie, T. Zhao, H. Liu, E. De Clercq, C. Pannecouque, J. Balzarini, X. Liu, Design, synthesis and preliminary SAR studies of novel N-arylmethyl substituted piperidine-linked aniline derivatives as potent HIV-1 NNRTIs, Bioorg. Med. Chem. 22 (2014) 633–642.

[15] Y. Song, P. Zhan, Q. Zhang, X. Liu, Privileged scaffolds or promiscuous binders: a glance of pyrrolo[2,1-f][1,2,4]triazines and related bridgehead nitrogen heterocycles in medicinal chemistry, Curr. Pharm. Des. 19 (2013) 1528–1548.

[16] Y. Tian, D. Du, D. Rai, L. Wang, H. Liu, P. Zhan, E. De Clercq, C. Pannecouque, X. Liu, Fused heterocyclic compounds bearing bridgehead nitrogen as potent HIV-1 NNRTIs. Part 1: design, synthesis and biological evaluation of novel 5,7-disubstituted pyrazolo[1,5-a]pyrimidine derivatives, Bioorg. Med. Chem. 22 (2014) 2052–2059.

[17] L. Wang, Y. Tian, W. Chen, H. Liu, P. Zhan, D. Li, H. Liu, E. De Clercq, C. Pannecouque, X. Liu, Fused heterocycles bearing bridgehead nitrogen as potent HIV-1 NNRTIs. Part 2: discovery of novel [1,2,4]triazolo[1,5-a]pyrimidines using a structure-guided core-refining approach, Eur. J. Med. Chem. 85 (2014) 293–303.

[18] E.B. Lansdon, K.M. Brendza, M. Hung, R. Wang, S. Mukund, D. Jin, G. Birkus, N. Kutty, X. Liu, Crystal structures of HIV-1 reverse transcriptase with etravirine (TMC125) and rilpivirine (TMC278): implications for drug design, J. Med. Chem. 53 (2010) 4295–4299.

[19] D.J. Kertesz, C. Brotherton-Pleiss, M. Yang, Z. Wang, X. Lin, Z. Qiu, D.R. Hirschfeld, S. Gleason, T. Mirzadegan, P.W. Dunten, S.F. Harris,

A.G. Villasenor, J.Q. Hang, G.M. Heilek, K. Klumpp, Discovery of piperidin-4-yl-aminopyrimidines as HIV-1 reverse transcriptase inhibitors. N-benzyl derivatives with broad potency against resistant mutant viruses, Bioorg. Med. Chem. Lett. 20 (2010) 4215—4218.

[20] (a) Y. Song, W. Chen, D. Kang, Q. Zhang, P. Zhan, X. Liu, "Old friends in new guise": exploiting privileged structures for scaffold re-evolution/refining, Comb. Chem. High. Throughput Screen 17 (2014) 536—553;
(b) D. Kang, Y. Song, W. Chen, P. Zhan, X. Liu, "Old dogs with new tricks": exploiting alternative mechanisms of action and new drug design strategies for clinically validated HIV targets, Mol. Biosyst. 10 (2014) 1998—2022.

[21] (a) C.M. Richardson, D.S. Williamson, M.J. Parratt, J. Borgognoni, A.D. Cansfield, P. Dokurno, G.L. Francis, R. Howes, J.D. Moore, J.B. Murray, J.B. Murray, A. Robertson, A.E. Surgenor, C.J. Torrance, Triazolo [1,5-a] pyrimidines as novel CDK2 inhibitors: protein structure-guided design and SAR, Bioorg. Med. Chem. Lett. 16 (2006) 1353—1357;
(b) N. Zhang, S. Ayral-Kaloustian, T. Nguyen, J. Afragola, R. Hernandez, J. Lucas, J. Gibbons, C. Beyer, Synthesis and SAR of [1,2,4]triazolo[1,5-a]pyrimidines, a class of anticancer agents with a unique mechanism of tubulin Inhibition, J. Med. Chem. 50 (2007) 319—327.

[22] (a) P. Zhan, Z. Li, X. Liu, E. De Clercq, Sulfanyltriazole/tetrazoles: a promising class of HIV-1 NNRTIs, Mini. Rev. Med. Chem. 9 (2009) 1014—1023;
(b) Y. Song, P. Zhan, X. Liu, Heterocycle-thioacetic acid motif: a privileged molecular scaffold with potent, broad-ranging pharmacological activities, Curr. Pharm. Des. 19 (2013) 7141—7154.

[23] H.M. Berman, J. Westbrook, Z. Feng, G. Gilliland, T.N. Bhat, H. Weissig, I.N. Shindyalov, P.E. Bourne, The protein data bank, Nucleic. Acids. Res. 28 (2000) 235—242.

[24] URL: http://www.certara.com/products/molmod/surflex/surflex-dock/.

[25] M.M. Hann, Molecular obesity, potency and other addictions in drug discovery, MedChemComm 2 (2011) 349.

[26] I. Weuts, F. Van Dycke, J. Voorspoels, S. De Cort, S. Stokbroekx, R. Leemans, M.E. Brewster, D. Xu, B. Segmuller, Y.T. Turner, C.J. Roberts, M.C. Davies, S. Qi, D.Q. Craig, M. Reading, Physicochemical properties of the amorphous drug, cast films, and spray dried powders to predict formulation probability of success for solid dispersions: etravirine, J. Pharm. Sci. 100 (2011) 260—274.

[27] C. Pannecouque, D. Daelemans, E. De Clercq, Tetrazolium-based colorimetric assay for the detection of HIV replication inhibitors: revisited 20 years later, Nat. Protoc. 3 (2008) 427—434.

[28] R. Pauwels, J. Balzarini, M. Baba, R. Snoeck, D. Schols, P. Herdewijn, J. Desmyter, E. De Clercq, Rapid and automated tetrazolium-based colorimetric assay for the detection of anti-HIV compounds, J. Virol. Methods 20 (1988) 309—321.

[29] Reverse Transcriptase Assay, Colorimetric kit, Roche Diagnostics GmbH, Roche. Applied Science, Sandhofer Strasse 116, D-68305 Mannheim, Germany.

[30] K. Suzuki, B.P. Craddock, N. Okamoto, T. Kano, R.T. Steigbigel, Poly A-linked colorimetric microtiter plate assay for HIV reverse transcriptase, J. Virol. Methods 44 (1993) 189—198.